RPN79

RADIATION PROJECT PROGRESS REPORT NUMBER 6

# MEASUREMENT OF BREMSSTRAHLUNG RADIATION PRODUCED WITH HIGH-CURRENT DIODES AND COAXIAL BLUMLEIN GENERATORS

by

JOHN J. CONDON

Electron Beams Branch
Plasma Physics Division

15 April 1969

Naval Research Laboratory
Washington, D. C.

## I. INTRODUCTION

This report summarizes a continuing effort to obtain a pulsed source of x-ray radiation. The portion of the work reported on here describes the progress made in diagnostics to measure spectra and energy fluence of the radiation field and development of field emission diodes for electron beam generation. The measured radiation quantities are compared with calculated values obtained with the ELECTREX program for the same conditions. Needle cathodes were used primarily as the electron source but recent emitters have been designed using vacuum-pinch and parapotential flow considerations.

The 50 nsec pulse for the electron gun was obtained with a 41-ohm oil blumlein coaxial generator. Calibration techniques for voltage probes to measure generator and tube voltage have been developed.

Both ionization chamber and thermoluminescent dosimeters were used to measure dose. X-ray spectra have been examined using absorption spectrometers employing film and TLD's as detectors of the transmitted radiation. Techniques have been developed to unfold the data so as to provide spectral information. The dependence of radiation on Z was determined by using anodes of titanium, molybdenum, and tantalum. Effect of tube voltage and current on the resulting radiation field was examined by measuring the intensity with a photodiode as a function of time.

## II. GENERATOR DESCRIPTION AND VOLTMETER CALIBRATION

### A. Generator

The 41.1-ohm folded coaxial blumlein generator using transformer oil as the dielectric is described in reference 1. This was the device

used to supply voltage for all of the electron gun experiments described here except for some recent experiments using a similar blumlein generator with water as a dielectric (see reference 2).

A typical intermediate voltage pulse shape is shown in Fig. 1a, for an open circuit condition without an electron gun in place. The upper trace is the signal from the voltmeter at the end of the intermediate pipe, which in this case represents a peak value of 295 kV. The positive portion represents the voltage on the intermediate pipe and the total change at the initial step is the open circuit or generator voltage. Ideally the generator voltage deflection would be twice the intermediate pipe value, but in Fig. 1a the measured ratio is 1.6. The bottom trace is the voltage on the center pipe using an $L \frac{di}{dt}$ loop later replaced by a capacitive voltage probe. Figure 1b shows the intermediate pipe signal and current for a short circuit condition.

B. Voltage and Current Measurement

The intermediate and inner or center pipe voltages were each measured separately with the same type of high-voltage capacitive probes described in reference 3. The current was detected by a $\frac{di}{dt}$ loop and the integrated signal measured on an oscilloscope. Calibration of this current loop was made by shorting the inner pipe at the output and then discharging the line. The resulting current signal can be displayed on an oscilloscope and compared to the calculated value which is found from the generator voltage (1.6x intermediate pipe voltage) and the line resistance of 41.1Ω.

Calibration of the capacitive voltage probes was made in three different ways. In all cases the probes were calibrated in situ, and during calibration of the output voltage probe (from the inner pipe),

the electron gun was mounted in place. The first two methods used dc and pulse charge calibration, and the third method employed rf techniques.

The dc calibration consisted in charging the pipe whose associated probe was to be calibrated, to about 25-35 kV as measured by an electrostatic voltmeter. The charged pipe was then shorted to ground and the resulting voltage pulse gave a coupled signal in the probe which was observed on an oscilloscope.

The pulse charge technique is similar to the one just described and is felt to be superior. It is fully described in reference 2. In both of these methods the accuracy of calibration is determined by the electrostatic voltmeter and oscilloscope accuracy, and is estimated to be 5-10%.

A third method uses an rf calibration technique in which the probe attenuation is compared with that of a known pad. A voltage, e.g. 10 volts, is supplied to the pipe to be calibrated and the resulting probe voltage is detected by a sensitive receiver (HP 310A wave analyzer). Since the voltage probe is in effect an attenuator which has a typical loss of 120-126 db, the loss from a calibrated attenuator could be substituted for the probe loss until the same voltage is detected by the receiver. The line capacitance of 2.5 nf is balanced by an inductance of 10$\mu$h at frequencies of 1 MHz to facilitate driving the system. This frequency is high enough not to affect the accuracy of the RC integrator and low enough not to make driving the high capacity of the line excessively difficult. In the calibrations that have been made, the attenuation could be resolved down to about 0.01db. In this technique it is not necessary to measure voltages but only to compare them. In the only comparison made thus far, the agreement between the dc calibration method and the rf technique was within 5%. In the use of this method shielding and leakage precautions are obviously important.

### C. Pulse Transformer

The voltage supply for the intermediate pipe was a pulse transformer whose primary was supplied by two Axel capacitors with a total capacitance of 1.1μf. The secondary consisted of 10 turns of RG-19 cable with the outer coax removed. The RG-19 cable with exposed polyethylene insulation was tightly wound on a 28-inch hollow cylinder of wood construction with adjacent turns pressed together. A single 10-inch wide copper strip was the primary. The previous operating limit for this pulse transformer was about 500 kV with a measured voltage step-up of 9.25. Modification of the design became necessary because of breakdown between adjacent turns on the secondary, after about the eighth turn, when voltages in excess of 500 kV were needed. Rather than use thicker insulation with larger cable it was decided to use more turns of the same RG-19 cable than had previously been used, thereby reducing the voltages between turns. The maximum number of turns was determined by the ratio

$$N^2 = \frac{\text{capacitance of storage capacitors } (1.1\mu f)}{\text{capacitance of generator } (2.5nf)}$$

N was calculated $\sim 23$.

In Appendix I the calculation procedure is outlined for determining the voltage step-up ratio for this 23-turn transformer.

## III. DIODES-BREMSSTRAHLUNG SOURCE

### A. Electron Gun Geometry

A parallel plane diode with a tungsten-needle-array cathode, described in reference 1, has been used for most of the experiments

during the past year with the 41-ohm generator. Recently, two types of solid-surface non-planar cathodes have been examined. In contrast to the needle cathode these employ a rather smooth surface of stainless steel which was sand blasted or plasma-torch-sprayed with tungsten. One of the cathodes has an emitting surface in the shape of a spherical cap; the other emitter has a conical surface (see Fig. 2a). The cone-shaped cathode has been designated as P-1.

These cathodes have all been used in a tube geometry of the type shown in Fig. 2b. Two tubes were used, the first having glass insulation with an effective length of 4.5 inches, which was increased to 5.75 inches in a second tube. This is the one currently in use. The original tube with the 4.5 inches of glass insulation had many pitting and crazing marks from sparking during a 50 ns pulse with peak voltages up to 500 kV. Although a corona ring was added externally to this tube it did not prevent the breakdown completely. In the second tube with the longer glass insulation no evidence of sparking has been observed for peak voltages up to 425 kV.

B. Emission Pictures

In addition to the current and voltage pulses which were measured for each discharge the diode performance was further checked by monitoring the electron emission using a closed circuit television. This procedure is described in detail in reference 1. A parallel magnetic field produced by an air-core solenoid used with the needle cathode provided a path for the electron flux from each emitter. The resulting radiation emanating from the anode is converted to visible light with a $CaWO_4$ intensifier screen which is placed against the back of the anode. The emission from the intensifier is observed with a television camera. It was determined that any separation between the anode and intensifier screen had to be prevented if information about the source of the radiation was to be accurate. For very thin

anodes, e.g. 5-mil thickness, which bowed in the middle because of atmospheric pressure, it was found necessary to use adhesive and to bond the screen to the back of the anode. Emission pictures were also obtained with the new solid-surface cathodes.

C. Molybdenum Anode - Needle Cathode

As described in reference 1 a parallel-plane diode configuration of needle cathode and molybdenum anode target with a spacing of 7/8-inch performed successfully without any evidence of breakdown for over 500 discharges. A typical example of the current and voltage pulse is shown in Figure 17 of the above reference. This was in contrast to the diode performance when titanium was the anode material, see Figs. 14 and 15 of reference 1. With the titanium material there were many breakdowns although the diode geometry and spacing were essentially the same as with molybdenum. On the assumption that the reasons given for the breakdown in the aforementioned reference were correct, i.e. hydrogen ion transit time, a very clean hard vacuum in the $10^{-9}$ mm Hg range was produced when the anode was changed from titanium to molybdenum.

After being in use about six months some of the vacuum-tight connections to the electron gun were disturbed and apparently a temporary leak was caused since it was subsequently noted that the pressure in the vacuum system was in the $10^{-7}$mm Hg range. The system pressure was finally reduced to the original $10^{-9}$mm Hg range but it is not known to what extent the apparent leak resulted in anode or cathode contamination.

Subsequent to this incident, breakdown became apparent, and after about ten discharges the current and voltage pulses of the type shown in Fig. 3a were obtained. This was apparently due to contamination

resulting from the leak in the system and again indicated the necessity for a very clean vacuum for non-breakdown discharges. Besides the gradually deteriorating tube performance as indicated by the current pulse, the observed emission via the closed-circuit television was very weak and came only from the stainless steel focusing collar, an example of which is shown in Figure 3b. The radiation as measured by the ion chamber was approximately 12 mr at two feet from the source or about 40% of what it had been.

The needles under microscopic examination did not show any marked differences as compared to new needles except that they might have been a little blunter. The needles were sharpened and cleaned by dipping them in a solution of NaOH before being returned to the electron gun.

The gas pressure increase in the vacuum system was monitored during discharge for this same run with the needle cathode and 0.010-inch molybdenum anode while the tube was still performing well. By using a mass spectrometer attached to the vacuum system of the electron gun it was found that hydrogen gas was responsible for the pressure increase during discharge. The identification was made on the basis that the amount of hydrogen present in the system was increased by 250 times during discharge and very little relative increase was measured for any other ion present in the system. The system pressure increased temporarily from the $10^{-9}$ mm Hg range to $10^{-7}$ mm but was quickly restored in a few minutes as the hydrogen was pumped back onto the anode surface.

D. Tantalum Anode - Needle Cathode

Subsequent to the run with the molybdenum anode, the electron gun referred to previously with the longer glass insulation of 5.75 inches between the internally mounted corona rings, was used for the

first time. Other changes made during this run were: The 0.010-inch molybdenum anode was replaced with 0.005-inch tantalum and the stainless-steel focusing collar mounted around the outside of the needle array was replaced with an otherwise similar anodized Al collar. The cathode-anode spacing was about 5/8-inch or about 1/4-inch less than before.

The 5-mil tantalum anode was perforated in three places from electron bombardment after two dozen discharges. Peak voltages during this run were about 312 kV. Minor difficulties prevented any emission pictures from being obtained with the closed circuit television before the tube failed, but other available evidence indicated that the Al collar did not have substantially less emission than the stainless steel. A Speed Graphic* camera was mounted several feet from the anode and a few pictures of the emission from the collar were obtained in this way. No emission was observed from the needles with this method. The solenoid field for the focusing lens, which was applied during a number of discharges, seemed to reduce the emission from the collar.

The vacuum side of the anode facing the cathode had a circle of severe pitting directly opposite the collar which also indicated a high electron flux from this source. The anode showed a definite pattern of works, resulting from melting and vaporization of metal, which corresponded to the locations of the needles in the cathode indicating that the needles were also emitting. Examination of the collar showed that the anodized insulation was broken through in several places to the underlying conductor surface. In the pictures, obtained with the camera, several points of rather intense emission were discernible in the bright ring of emission from the collar. It seems clear that the electron flow which caused the anode perforation emanated from these locations on the collar.

*Made by Graflex Inc., Rochester, New York.

Another run was made with a new 5-mil tantalun anode and the stainless steel collar was put back on. Examples of current and voltage pulses are shown in Fig. 4. The tube was still operating in a satisfactory manner after 28 discharges at peak voltages up to 425 kV, when the pulse transformer had a high voltage breakdown.

E. Dome-Shaped Cathode

The first of the solid surface cathodes was installed in the tube while the transformer was being repaired. A picture of this cathode is shown in the right-hand side of Fig. 2a. The shape of the emission surface of this cathode was a spherical segment, referred to as a "dome-shaped" cathode, with a maximum height of 1/8 inch. The minimum spacing between the 5-mil tantalum anode and the cathode was 0.466 inches. Voltage and current values were low with the diode, peak values of 312 kV, 3.7 kA were obtained (r=84.4 ohms) and were different shape from those obtained with the needle cathode. Examples are shown in Fig. 5a as well as cathode emission in Fig. 5b via closed circuit television. The performance of the tube during this run was erratic and although it seemed to improve as evidenced by the voltage pulse becoming more trapezoidal in shape, the radiation output kept decreasing as determined by the ion chamber measurements. After 39 discharges the cathode-anode spacing was changed to 0.215 inches.

A picture of the 5-mil tantalum anode removed from the tube when the spacing was changed is shown in Fig. 6. The surface shown is the one facing the cathode and the distinct ring of melting and vaporization has the diameter of a circle on the cathode face which was about 2 mm less than the cathode in radius.

The new diode spacing of 0.215 inches seemed to increase the tube resistance. For the first 20ns the voltage represented essentially an open circuit condition and had a peak value of 190 kV. When the

current value was about 1 kA the resistance had dropped to about 140 ohms and at a peak current of 2 kA the resistance had dropped to about 40 ohms.

F. Conical-Shaped Cathode

The first of a series of solid surface cathodes (designated as P-1) employing the concept of parapotential flow was next evaluated. It is shown in the center of Fig. 2a and discussed in detail in reference 4. (See also Fig. 4 of this reference.) Separation of the cone tip from the anode was 0.250 inches. Initially the anode was 5-mils tantalum, which was punctured in two or three discharges by the electron beam. Voltage was low, and for peak values of 104 kV the peak current was 7.7 kA. The resistance was changing during the pulse being about 23 ohms at the time of peak voltage. (See Fig. 7a.) A 15-mil titanium anode with the same cathode-anode separation gave a value 21.2 ohms of the time of peak current (16.3 kA). (See Fig. 7b.) Peak voltage was about 484 kV, occurring ahead of the peak current. The anode was punctured after six discharges. A third type of anode, 0.125 aluminum, replaced the titanium and on the third discharge the diode behaved as a nearly constant impedance device of 8.1 ohms and maximum current of 12.3 kA. (See Fig. 7c.)

Preliminary results were obtained with the second of these vacuum-pinch diodes (P-2) using the new 7-ohm generator with water dielectric. This was the first time that an electron gun was used on the new generator. A drawing of this diode is given in Fig. 10 of reference 4. Cathode tip-anode spacing is 0.125 inches for this version of the P-2 diode. The water switch on the intermediate pipe was only partially opened in these first discharges so that the

generator was not performing at full potential. Under this condition tube voltage was 370 kV maximum, with a peak current of 23 kA. The diode resistance at peak current was 12.3 ohm. (See Fig. 8) It should be remembered in all the pictures of current and voltage that the output voltage probe detects the voltage pulse before it reaches the electron gun and charge begins to flow. To compare current and voltage at the same time for such calculations as tube resistance the voltage trace should be moved to the right to correct for this time lapse. In Figs. 7 and 8 this correction is about 2 nsec.

## IV. RADIATION DIAGNOSTICS

An evaluation was made during the past year of the necessary techniques and data analysis needed to measure the radiation dose and spectrum of bremsstrahlung energy from a pulsed x-ray source. This has been accomplished by evaluating ion chamber design, photodiodes, photographic film, and thermoluminescent dosimeters (TLD), which are described in the following.

### A. Radiation Dose

Radiation dose measurements with ion chambers was improved during the year by constructing a 20 x 20 inch cylinder with Al walls 0.125 inches thick. It was evacuated and baked out and then filled with neon gas to 1 atmosphere pressure. The neon gas used at this time had 1% methyl formate impurity. The use of a non-electron-attaching gas would avoid recombination of ions and be an improvement of the two air chambers previously used, see reference 1. The collector plate was centrally located with a 1500 volt potential. The uncorrected calibration constant for this chamber is 17 joules/$cm^2$ coulomb. An RC integrated current was measured with an oscilloscope across a 10-megohm viewing resistor.

To check the accuracy of the calculated calibration constant and provide a second independent measurement of radiation dose a method utilizing thermoluminescent dosimeters (TLD) was devised. The dosimeter bulbs were mounted in cylindrical cases which are called filters. In a typical run four different TLD filter combinations were mounted two feet from the source, exposed to a pulse of radiation, and then removed. This procedure was repeated four times and an average value obtained for each dosimeter-filter combination. The generator was charged to approximately the same voltage each time and has been very repeatable in its pulse output so that nearly the same radiation field was produced for each discharge. The current and voltage to the diode and the ion chamber signal were measured for each pulse.

$CaF_2$ and LiF were the thermoluminescent materials that were used in the glass bulb dosimeters. Each of the two materials was used with and without shielding, which gave a total of four measurements of the radiation field. These uncorrected dosimeter readings are all different even though they are exposed to the same radiation flux, and have to be corrected by using the response curve for each dosimeter-shielded combination in conjunction with the energy spectrum of the radiation field. Ideally, of course, when the four values are so corrected they will yield the same dose since they are exposed to the same radiation field. This was the criterion used in the calculation procedure outlined in Appendix II and discussed in reference 5. These computation steps have been written into a short computer program called "Confluence".

The radiation energy as measured by both the ion chamber and the TLD's was compared for titanium, molybdenum, and tantalum converter anodes and is summarized in Table I. The flux produced by the 15-mil titanium with peak electron energy values of 480 kV was measured with an ion chamber filled with air at 1 atmosphere

pressure and $CaF_2$ dosimeters. The dose measured by the chamber was about one-half of that determined by the dosimeters. A similar comparison was made using a 10-mil molybdenum converter with electrons having a peak energy of 450 kV. The radiation energy was measured by the new neon ionization chamber and $CaF_2$ and LiF dosimeters. The dosimeter values were corrected in the manner referred to above and the agreement among the dosimeters and the neon chamber was very good. In a more recent comparison 7(508), a 5-mil tantalum anode was used and about 2-1/2 times less radiation was indicated by the ion chamber as compared to the dosimeter value. It is probable that the oxygen content of the neon gas increased since it was put into the chamber. The effect of impurities has been examined by measuring the same dose with two identical chambers, one filled with 99.998% pure neon gas at 4 psig and the original chamber refilled with the less pure neon gas containing 1% methyl formate, also to 4 psig. An example of the measured signals from each chamber is shown in Fig. 9, which shows that each gas has about the same signal rise time, but the dose measured by the less pure neon is about 15-30% less than the dose using the very pure neon gas. See also number 615 and number 7 in Table I for the actual dose values. These results show that the radiation measured by the ion chamber is very sensitive to the purity of the neon gas. The neon used prior to refilling produced a long rise time suggestive of the presence of electron-attaching impurities.

In Table I the large difference in the dose measured by the TLD's and ion chamber as given by 7(508) will be resolved by further calibration. The low efficiency for the P-2 cathode determined by No. 7 will have to be re-examined by obtaining additional data.

B. Photon Spectra

Techniques in the measurement of continuous photon spectra have received additional evaluation during this year by using both

photographic film and thermoluminescent dosimeters as the radiation detectors in absorption spectrometers. A description of the film spectrometer and the calculation procedure used to invert the absorption matrix and yield an energy spectra is given in reference 6.

The least square procedure outlined in Appendix III of the above reference for comparing a calculated intensity to the measured intensity based on assuming an initial energy spectrum, has received additional refinements. A new absorption coefficient matrix was obtained in which an average value over 50 keV increments was obtained by integration. This proved to be more accurate than the previous mean average that was used. Another improvement was to use better values for the coefficients which were obtained from McMasters' data.

In addition to these improvements, different types of film were exposed to the radiation transmitted through Cu or Pb filters of the absorption spectrometer, and the energy spectrum obtained with each type of film were compared. For this comparison the radiation was approximately the same in all cases, originating from a molybdenum converter anode 0.010 inches thick, with the spectrometer located two feet from the source. Although there was some variation in peak accelerating voltages it was expected that by exposing each film a number of times, an average sample of radiation would be seen by the film. Agfa Isopan Record and Kodak 2475 recording film were used in addition to the Kodak Trix-X film. These three types cover a wide range in film speed.

The film was developed according to manufacturer's instructions and the relative intensity for each Cu and Pb filter was measured using a Joyce Lobel densitometer. The recorder displacement for each filter was compared to the displacement representing maximum transmitted light intensity and the logarithm of the ratio was normalized with

respect to the Al filter. This constituted the experimentally measured intensity and by using this in conjunction with the least square procedure an energy spectrum was derived.

The energy spectra obtained with molybdenum converter were in qualitative agreement for the different types of film. The variation was confined primarily to the lowest energy interval considered i.e. 50 keV and for higher energies the quantitative agreement was rather good. The agreement was best when the second or third iteration was used, after which the individual values started to vary widely. This is due to error in the measured intensities and to degeneracy in the absorption matrix. Typical results for the three films are shown in Fig. 10.

A modification of this technique consists in replacing the film by thermoluminescent dosimeters (TLD) as detectors of the filtered radiation. This TLD spectrometer is a four-inch square box, partitioned into twelve compartments where the TLD bulbs could be placed. The front of the box facing the radiation was formed by filters of identical thickness to those used in the film spectrometer, see Fig. 11a.

Two runs have been made with this spectrometer using LiF as the fluroescent material. As shown in Fig. 21 (Appendix II) the response curve for LiF is not flat but as a first approximation it was assumed to be. The ratio of the filtered to the unfiltered dosimeter readings were formed and these normalized values were used as the measured spectra in the least squares calculation procedure previously referred to. Two spectra have been measured in this way, one for 0.010-inch molybdenum and the other for 0.005-inch tantalum. The derived spectrum for molybdenum (see Fig. 12) is in reasonably

good agreement with the film results shown in Fig. 10. No spectra were obtained with the film spectrometer for tantalum.

Another method of deriving the spectra from these TLD spectrometer measurements is to extend the calculation procedure outlined in Appendix II. This procedure was originally derived for obtaining radiation dose from dosimeter measurements as described in Part A of this section and is useful only if one has reasonable knowledge of the spectrum initially. Since the same type of data is available when the dosimeters are exposed to the filtered radiation in the spectrometer it is only necessary to add additional response curves for the new filter and bulb combinations in order to use the same calculation procedure.

From initial results with the box-type TLD spectrometer (see Fig. 11a) it was suspected that radiation from filters adjacent to a particular compartment could reach the dosimeter bulb. This is now avoided by use of another spectrometer design where each filter is a hollow cylinder in which the dosimeter is placed and whose wall thickness corresponds to the earlier flat filter thickness, see Fig. 11b. In this way the bulbs are only exposed to radiation filtered through the same thickness of either lead or copper. The dose and spectra obtained with the box-type TLD spectrometer is compared with calculated values in Section V.

### C. Unattenuated Kramers Spectra

A method was developed for obtaining a spectrum for the range of electron energies in a pulse by use of Kramers's Rule to provide an approximate spectrum neglecting target absorption. This spectrum takes account of the decay in electron energy in the

target. The oscilloscope pulse shapes of current and voltage are measured at the same instant of time during the 50 nanosecond pulse. Typically the interval is divided into 10 increments. This step can be facilitated with an x-y plotter by making negatives of the polaroid prints and using a photomultiplier readout device to plot current and voltage curves permitting the amplitudes to be read directly. Since the current is proportional to beam intensity, and voltage to energy, a family of straight lines are plotted assuming a Kramers spectrum. Each pair of current and voltage values represent a line whose slope is determined by the current, and the intercept value on the abscissa is given by the magnitude of the voltage. The family of lines generated in this manner intersected with one another and the ordinate values of the intersection points were summed at the same voltage and plotted as spectra. The plotting and summation were facilitated with a short computer program. An example of the final unattenuated, concave shaped spectra generated in this way with energy values between 0 and 500 keV is shown in Fig. 13.

By using this unattenuated energy spectrum in conjunction with measured TLD values and their response functions, a photon energy spectrum was produced by taking into account the radiation absorption in the target. This procedure is discussed in reference 5 and outlined in Appendix II. Examples of spectra generated by this method are given in Figs. 16-18.

D. Photodiode

The time-dependence of the radiation on the current and voltage to the x-ray tube was determined with a photodiode, whose response is directly proportional to the radiation intensity. A high-current biplanar phototube* was placed in a copper cylinder

*The FW-114 diode was obtained from the ITT Industrial Laboratories.

along with a scintillator and covered with a thin Al window to prevent any visible light from entering. The scintillator was a one-inch-thick cylinder of pilot B which was placed directly against the glass face of the diode with a thin layer of grease. The anode screen was connected to a 2000-volt supply through a 1000-Ω isolation resistor and a 0.002μf capacitor to ground. A helical membrane shielded cable connected the cathode to the oscilloscope for measuring the voltage signal from the collector plate.

A relationship between the current and voltage and photodiode signals as shown by the following proportionality

$$\frac{(\text{photodiode})_1}{(\text{photodiode})_2} \propto \frac{(iV^3)_1}{(iV^3)_2}$$

was found to be approximately correct. A numerical example of this relationship is given by

$$\frac{24 \text{ units}}{8 \text{ units}} \propto \frac{3(2^3) \text{ units}}{8(1^3) \text{ units}}.$$

The subscripts 1 and 2 refer to the times corresponding to peak voltage ($t_1$) and peak current ($t_2$).

The quantity $iV^3$ can be interpreted as the product of the power into the electron beam or iV, multiplied by the conversion efficiency given as $\sim V^2$. This dependence is valid for intermediate Z targets at primary electron energies of $\sim$ 400 keV, and takes account of photoelectric absorption. Then the product of beam power x efficiency is given as $iV^3$.

### E. Other Diagnostics

In addition to the previously discussed diagnostics it had been planned to measure the temperature rise in the anode converter by monitoring a thermocouple response and to relate this to the incident beam energy and energy in the radiation field. A chromel-alumel thermocouple was soldered to the back of the anode, but due to electrical noise it proved to be unsatisfactory. Further efforts were postponed and a calorimeter was designed and built to determine the energy profile of the electron beam by measuring the temperature rise of carbon blocks with thermocouples imbedded in them, see Fig. 14a. This calorimeter will be positioned inside a partially evacuated drift tube which has been designed to fit the end of the electron gun used with the 7-ohm generator, see Fig. 14b. The 7-ohm generator has recently been completed and is described in reference 2. A high-current (upwards of 70 kA) beam should be available with this generator and the drift tube and calorimeter experiments will begin in the near future.

## V. COMPARISON OF THEORY AND EXPERIMENT

Photon spectrum and dose as determined by theory and experiment are compared for three anode converters of different Z, which are 15-mil titanium, 10-mil molybdenum, and 5-mil tantalum. The current and voltage, ionization chamber, and TLD measurements were obtained in each case so that a detailed comparison is possible. The theoretical results are those determined with the ELECTREX computer program. Initial description of this code was given in reference 1, and will be fully described in a forthcoming report. Continual improvements are being made such as incorporating the most recent absorption cross section data, increasing the energy range of applicability, and modifying the program input to accept an actual

primary electron energy spectrum instead of a single primary electron energy. This last improvement will allow a very close comparison to be made with experimentation since the simultaneous measurement of current and voltage permit the actual beam energy spectrum to be used in the calculation.

The experimental spectra in the following comparison have all been determined by means of TLD measurements which were corrected by the procedure described in Appendix II using program "Confluence".

The ELECTREX results were determined for actual primary electron energy spectra which were calculated by a subroutine called SPECTOR from the measured current and voltage values determined by the oscilloscope traces. The three electron beam spectra are shown in Fig. 15 a,b,c for the actual runs being considered 1(45), 4(256), 7(508) which are for the titanium, molybdenum, and tantalum converters respectively.

The spectra for titanium, molybdenum, and tantalum are shown in Figs. 16-18. Agreement at the low energy end and at the peak values is good in all cases, although at the higher energy the spectra determined experimentally are shifted to the right of the calculated curve, indicating that more energetic photons appear to be present than there are calculated to be. The spectral shapes given by the results are really determined by the initial Kramers spectrum and the theoretical absorption figures, so that the soft-end agreement with ELECTREX is not surprising. The TLD outputs are in fact not exceedingly sensitive to spectral shape. In view of the many uncertainties in the experimental spectrum measurements, it is presently felt that, if the primary electron spectrum is known, the code furnishes the best obtainable information concerning spectrum and efficiency. The hard-end agreement is in fact better between the direct

TLD absorption measurements (Figs. 10 and 12) and the code than what the Kramers spectrum provides.

Comparison of measured and calculated dose requires a known value of electron beam energy since the quantity determined in the ELECTREX program is the conversion efficiency of electrons to photons. Since the instantaneous current and voltage are known, the beam energy is readily determined by graphically representing the beam power as a function of time and integrating. The graphical integration for the titanium, molybdenum, and tantalum converters, gave values of 100, 60, and 90 joules, respectively. The run numbers of 1(45), 4(256), and 7(508) which are used here are also referred to in Table I which gives the dose values at two feet from the source. If the radiation is assumed isotropic within a hemisphere a two-foot radius (A=23, 400 $cm^2$) then the total radiation energy can be found and compared to the beam energy, permitting an efficiency to be determined which can then be compared to the value calculated by the ELECTREX program. These results are shown in Table II where the TLD dose values previously given in Table I are used in this comparison.

The values of thickness used in the different converters are not meant to be optimum thicknesses from the point of conversion efficiency. They were selected as a good thickness to begin with, which could be refined at a later time. A separate routine in the ELECTREX program does calculate the optimum thickness but no work has been done on this experimentally.

The calculated efficiency as a function of converter thickness is shown in Figs. 19 and 20 for titanium, molybdenum, tantalum, and uranium. These values were provided by a subroutine of the ELECTREX program and are for monochromatic electrons of

500 keV energy. The efficiency values shown by these plots are higher than those given in Table II, for these same converter materials, since those were for the actual electron spectra used.

It is planned to make a similar comparison to that shown in Table II for the case of uranium converter material using the P-2 diode and the 7-ohm generator. Delays in obtaining the depleted uranium discs have made it impossible to include this here.

## APPENDIX I

### Calculation of Voltage Step-Up Ratio for a Pulse Transformer

The circuit for the 23-turn pulse transformer, which provided the voltage for the 41-Ω oil blumlein, can be represented as

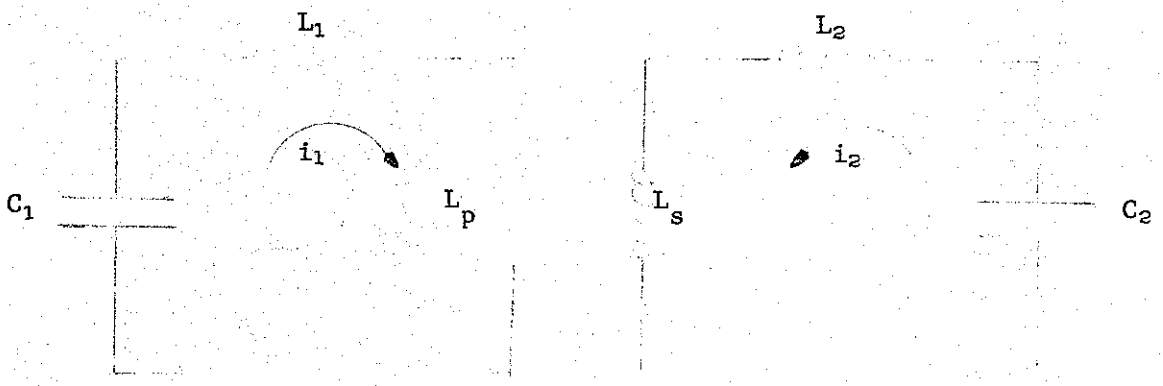


where $C_1$ = Axel capacitor storage = $1.1 \times 10^{-6}$f

$C_2$ = Blumlein capacitance = $2.5 \times 10^{-9}$f

$L_1$ = Switch inductance = $0.081 \times 10^{-6}$h

$L_2$ = Generator inductance = $0.0428 \times 10^{-6}$h

$L_s$ = Secondary inductance = $Fn^2d$ (p. 53 and 54 Terman*)

$L_p$ = Primary inductance = (p. 53 and 54 Terman*).

The derivation is easiest in terms of reduced coupling coefficient

$$k' = k\sqrt{\frac{L_s L_p}{L_s' L_p'}} \quad , \quad L_p' = L_p + L_1 \, , \; L_s' = L_s + L_2$$

*Radio Engineers Handbook - Terman

where

$$k = \frac{M}{\sqrt{L_p L_s}} \text{ (Pg. 71 Terman).}$$

Then $V_1 = z_{11} i_1 + z_{12} i_2$

$V_2 = z_{12} i_1 + z_{22} i_2$ and the normal mode frequencies are bound to be

$$\omega_{1,2}^2 = \frac{1}{2(1-k'^2)} \left[ (\omega_s^2 + \omega_p^2) \pm \sqrt{(\omega_s^2 - \omega_p^2)^2 + 4k'^2 \omega_s^2 \omega_p^2} \right]$$

where

$$\omega_s^2 = \frac{1}{C_2 L_s'} \quad , \quad \omega_p^2 = \frac{1}{C_1 L_p'} \quad .$$

The voltage step-up ratio $\frac{V_2}{V_1}$ is found to be

$$\frac{V_2}{V_1} = k' C_2 \sqrt{L_p' L_s'} \sqrt{(\omega_s^2 - \omega_p^2)^2 + 4k'^2 \omega_s^2 \omega_p^2} \qquad (\cos \omega_1 t - \cos \omega_2 t)$$

where $V_1$ is the d.c. voltage on $C_1$ and $V_2$ is the voltage across $C_2$ as a function of time.

In calculating $L_s$ and $L_p$ the value for F was determined by the ratio $\frac{\text{diameter}}{\text{length}}$ of primary or secondary and Table 12 in Terman. The values used were

$$\frac{d_s}{l_s} = \frac{28.36''}{20.8''} = 1.34; \frac{d_p}{l_p} = \frac{28.63''}{20.5''} = 1.40.$$

As mentioned in Section I, $\frac{V_2}{V_1} = 16.20$ by this calculation and was measured to be 9.25. The ratio of the periods $\frac{T_1}{T_2}$ for the normal frequencies $\omega_{1,2}$ was calculated to be 3.41 and was in good agreement with the experimental value.

## APPENDIX II

### Calculation Procedure for Determining Radiation Dose and Spectra from TLD Exposures

This is an outline of the procedure shown in greater detail in reference 5. The first step is to correct an unattenuated Kramers spectra for absorption in the target. As a beginning any spectrum could be used. The unattenuated Kramers spectrum was described previously in Section IV and was obtained with simultaneous current and voltage pulses from a family of Kramers-type curves assuming that at any instant a straight line spectrum is being generated. The correction factor is provided by computing $\frac{I}{I_o} = e^{-\mu x/\rho}$ for various energy values ($\mu$ a function of energy) at a given thickness of converter. The product of this correction factor and the computed unattenuated spectrum for different energies is the attenuated energy spectrum. Different thicknesses of converter are chosen which are some fraction of the total thickness. It is assumed that the conversion all occurs at the thickness chosen and that the radiation is then filtered by the remaining converter thickness. For example, if it is assumed as a first approximation that the radiation is generated at 0.5 of the anode thickness the remaining 0.5 thickness would attenuate the radiation.

The second step is to use this approximate attenuated spectrum and dosimeter response curves to calculate a "weighting" function correction to be applied to the uncorrected dosimeter readings. This is necessary since both the response curves and the radiation field are energy dependent. Examples of the response curves are shown in Fig. 21. Multiply each dosimeter response function by the attenuated spectrum and integrate the product from 30 to 500 keV. In multiplying, an average value of each quantity over an interval of energy is chosen, say 50 keV intervals. Integrate the area under the attenuated spectra and divide this into the previous result.

The number obtained is the correction factor for that particular dosimeter and shield combination. For the example being considered here there were four response functions, one for each of the four dosimeter and shield combinations used,a calcium fluoride bulb and a lithium fluoride bulb with and without shields.

The next step is to correct the actual TLD reading for each dosimeter and filter by dividing it by the above correction factor, and obtain the x-ray energy fluence in ergs/$cm^2$. An average fluence value can then be obtained for the corrected dosimeter readings and the standard deviation obtained for these readings. Ideally, this corrected dosimeter reading would be the same for each dosimeter since they are each measuring the same radiation field and if properly corrected must give the same result. The fact that they don't measure the same radiation value means that the attenuated spectra needs additional refinement.

The above steps are repeated for other choices of target thicknesses e.g. 0.3, 0.4, 0.6, 0.7 of the distance from the exit fact. The standard deviation is plotted as a function of target thickness and a minimum value obtained. The converter thickness associated with the minimum standard deviation is used to calculate an attenuated spectrum and dose by repeating the steps outlined above. A program called "Confluence" is used to do these calculations for a given unattenuated spectrum, dosimeter readings and response functions.

The "TLD Spectrometer" described in Section IV is just a generalization of the foregoing, from the case of four dosimeter response curves to a half-dozen or more. Lithium fluoride is the material used in all the dosimeters and it is expected that spectra obtained in this way will have a higher resolution than that obtained by just using four response curves.

## REFERENCES


1. J. J. Condon, D. C. dePackh, J. B. Ehrman, and J. D. Shipman, Jr., "Interim Report on X-Ray Techniques Project," NRL Report 6671, S/RD, January 30, 1968.

2. J. D. Shipman, Jr., "A 7-Ω, 1-mV, 50-nsec Water Dielectric Pulse Generator," September 1968, Radiation Project Progress Report Number 8.

3. G. Leavitt, J. D. Shipman, Jr., and I. H. Vitkovitsky, Rev. Sci. Instr. 36, 1371 (1965).

4. D. C. dePackh, "Parapotential Flow," Radiation Project Progress Report Number 5, June 24, 1968.

5. F. Attix, J. J. Condon, and A. Nash, "Estimation of Bremsstrahlung Spectra and Energy Fluence from Pulsed X-Ray Generators," (to be published).

6. D. C. dePackh, "Absorption Spectrometer," Radiation Project Internal Report Number 2, 12 October 1967.

## TABLE I

## EXPERIMENTAL DOSE MEASUREMENTS

### Source - 15-mil Ti (Needle Cathode)

1(46)

| TLD Type | ergs/cm$^2$ | Ion Chamber |
|---|---|---|
| (U)$CaF_2$ | 80.0 | Gas - Air |
| (S)$CaF_2$ | 81.1 | Pressure - 1 atmosphere |
| Avg | 80.5 ± 1% S.D. | Energy - ~ 37 ergs/cm$^2$ |

### Source - 10-mil Mo (Needle Cathode)

4(256)

| TLD Type | ergs/cm$^2$ | Ion Chamber |
|---|---|---|
| (U)$CaF_2$ | 86.9 | Gas - Neon |
| (S)$CaF_2$ | 73.8 | Pressure - 1 atmosphere |
| (U)LiF | 90.1 | Energy - 97.5 ergs/cm$^2$ |
| (S)LiF | 96.6 | |
| Avg | 86.85 ± 9.39% | |

### Source - 10-mil Mo (Needle Cathode)

5A(409)

| TLD Type | ergs/cm$^2$ | Ion Chamber |
|---|---|---|
| Spectrometer: | 133 ergs/cm$^2$ ± 13.4% | Gas - Neon |
| | | Pressure - 1 atmosphere |
| | | Energy - 41.4 ergs/cm$^2$ |

## TABLE I (Continued)

### Source - 5-mil Ta (Needle Cathode)

7(508)

TLD

| Type | ergs/cm$^2$ |
|---|---|
| (U)$CaF_2$ | 563 |
| (S)$CaF_2$ | 554 |
| (U)LiF | 627 |
| (S)LiF | 581 |
| Avg | 581 ± 5.6% S.D. |

Ion Chamber

Gas - Neon

Pressure - 1 atmosphere

Energy - 239 ergs/cm$^2$

### Source - 5-mil Ta (Needle Cathode)

7A(508)

TLD

Type ergs/cm$^2$

Spectrometer: 650 ergs/cm$^2$ ± 15% S.D.

Ion Chamber

Gas - Neon

Pressure - 1 atmosphere

Energy - 239 ergs/cm$^2$

Remarks: Impurity content of gas in ionization chamber may have increased.

### Source - 15-mil Ti (P-1 Cathode)

(615)

TLD

Type ergs/cm$^2$

(None was used)

Ion Chamber

Gas - Neon

Pressure - 4 psig

Energy - (ergs/cm$^2$) 90[a] 106[b]

Remarks: New gas in both chambers: (a) neon gas impurity 1% methyl formate
(b) 99.998% pure neon gas

## TABLE I (Continued)

### Source - 5-mil Ta (P-2 Cathode)

### (7)

| TLD | | Ion Chamber |
|---|---|---|
| Type | ergs/cm$^2$ | |
| (None was used) | | Gas - Neon |
| | | Pressure - 4 psig |
| | | Energy - (ergs/cm$^2$ 59[a] 85[b] |

Remarks: New gas in both chambers (a) neon gas impurity 1% methyl formate
(b) 99.998% pure neon gas

In Table I the TLD and Ion Chamber values are both given at two-feet from the source. (U) - Unshielded dosimeter, (S) - Shielded dosimeter.

TABLE II

CALCULATED AND MEASURED RADIATION DOSE

| Run No. | Converter | TLD Dose ergs/cm$^2$ | Total Radiation Energy-Joules | Beam Energy Joules | Efficiency % | Calc. Effi. ELECTREX % |
|---|---|---|---|---|---|---|
| 1(45) | 15-mils Ti | 80.5 | 0.188 | 90 | 0.24* | 0.25 |
| 4(256) | 10-mils Mo | 87.0 | 0.204 | 60 | 0.34* | 0.25 |
| 7(508) | 5-mils Ta | 581.0 | 1.36 | 100 | 1.36* | 0.42 |

*The values shown for experimental efficiency are estimated to be ±25%. As discussed in the text, the experimental methods are being investigated further in order to obtain more precise information that will be more nearly in agreement.

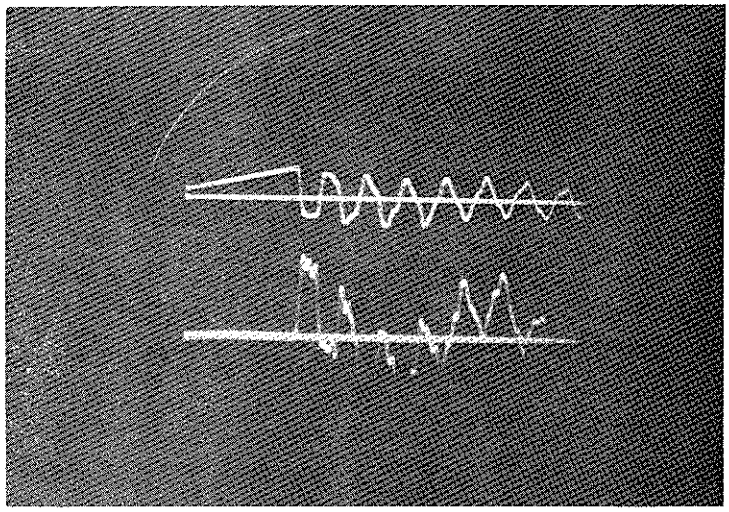

Figure 1a - Open circuit condition. Top trace - intermediate pipe 295 kV. Lower trace - center pipe voltage.

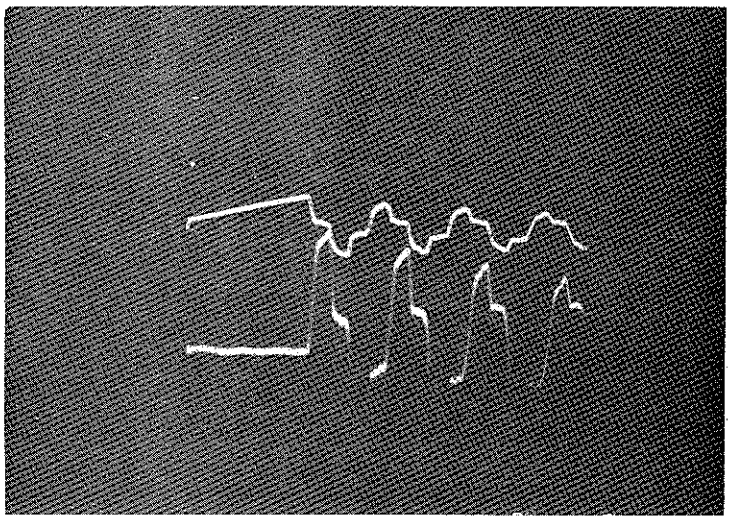

Figure 1b - Short circuit condition. Top trace - intermediate pipe voltage. Lower trace - current.

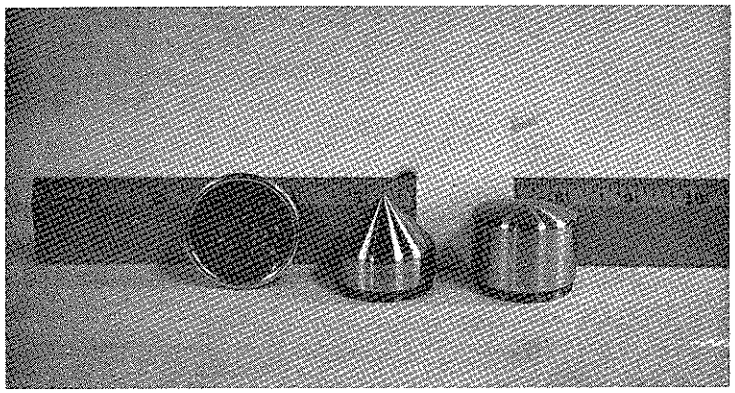

Figure 2a - Left, original 50-needle cathode with stainless steel collar. Center, new cone-shaped cathode (P-1). Right, dome-shaped cathode (prior to sand-blasting).

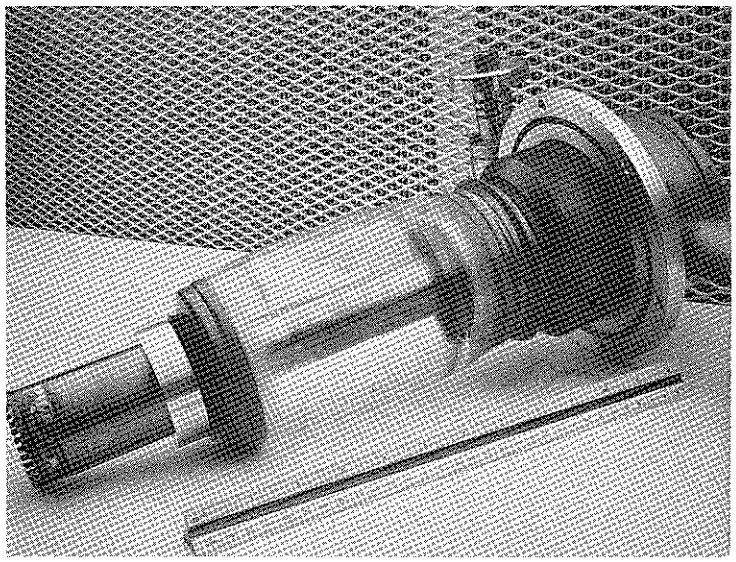

Figure 2b - Electron gun used with the cathodes shown in Figure 2a

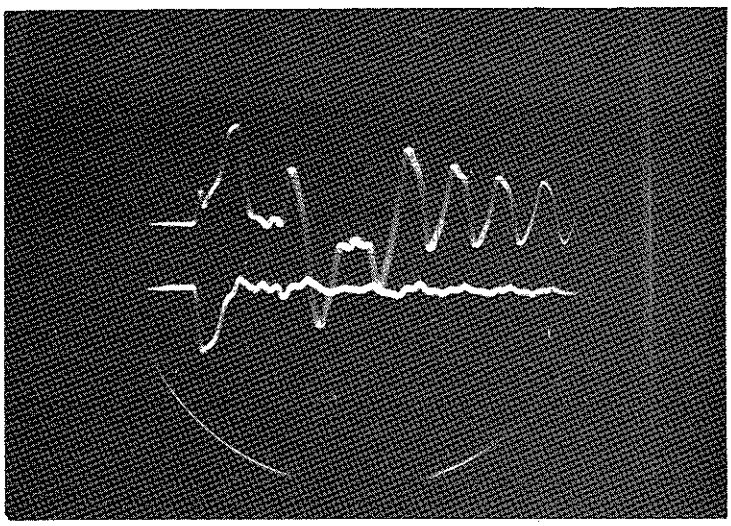

Figure 3a - Current (10.6 kA max) and voltage (550 kV max) after presumed contamination of Mo anode and needle cathode

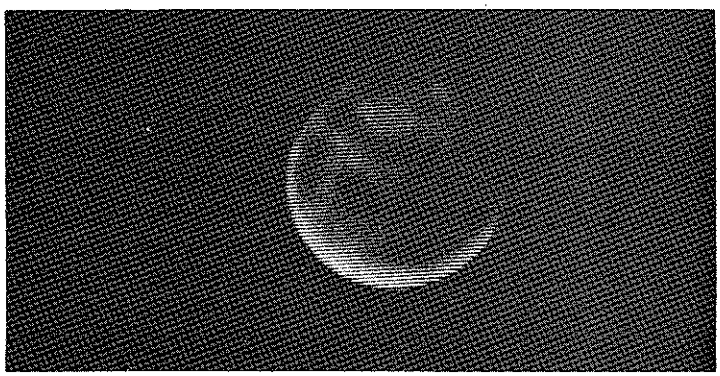

Figure 3b - Typical picture of emission after presumed diode contamination

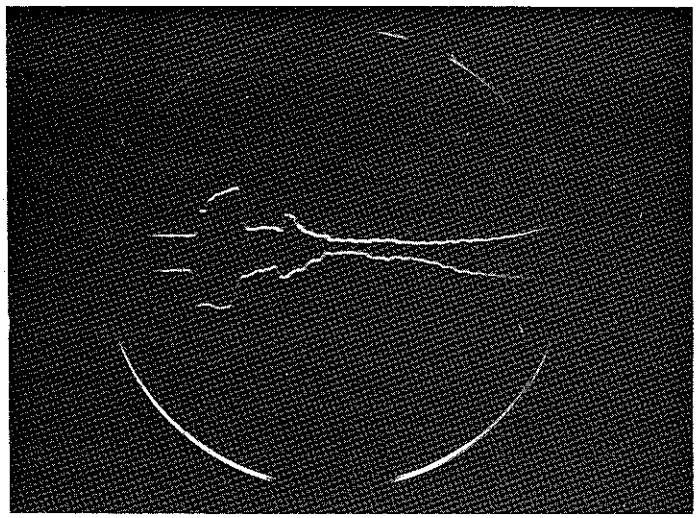

Figure 4 - Current (top trace) and voltage for needle cathode and tantalum anode. Spacing 5/8 inch. i(max) = 5.1 kA. v(max) = 312 kV.

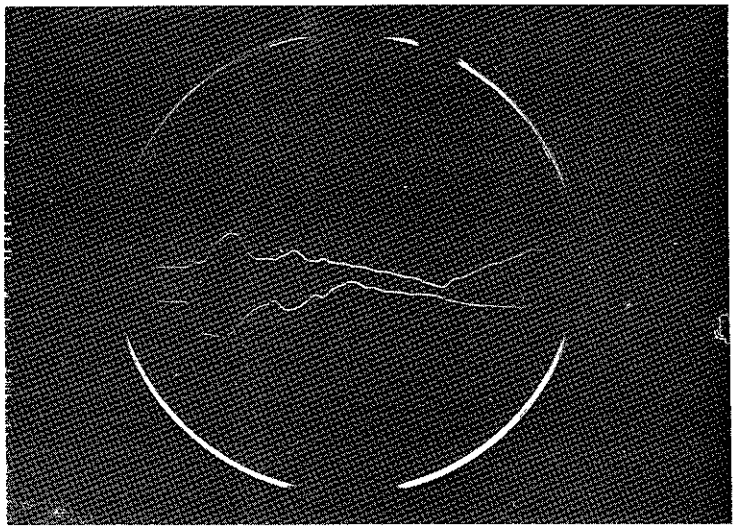

Figure 5a - Current (upper trace) and voltage with "dome-shaped" cathode and tantalum anode. Spacing 0.466 inches. i(max) = 3.7 kA, v(max) = 312 kV.

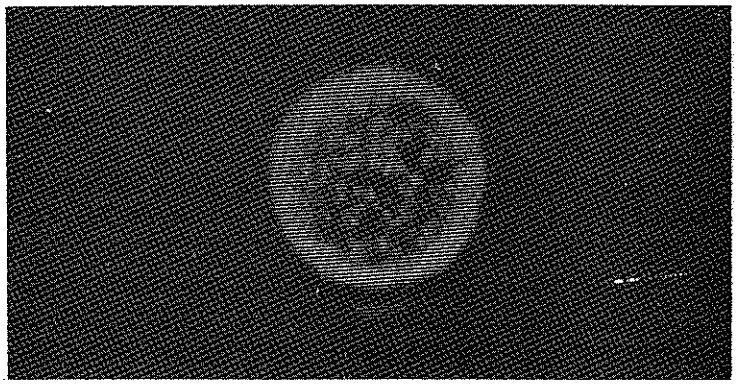

Figure 5b - Emission from "dome-shaped" cathode

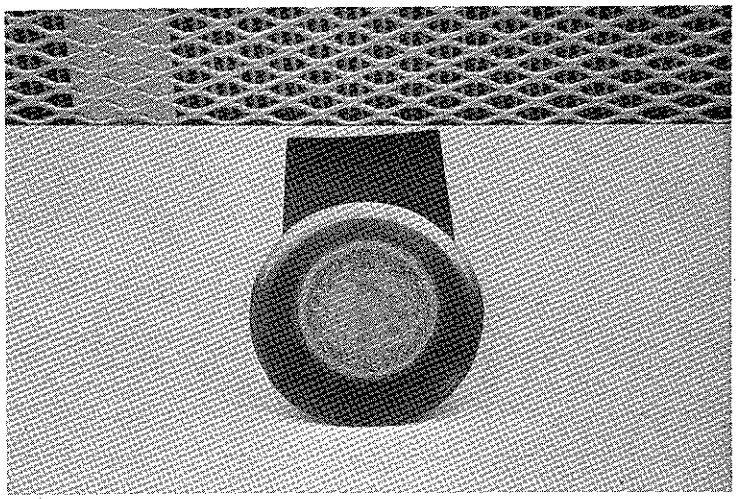

Figure 6 - Photograph of 5-mil tantalum anode used with dome cathode. Minimum separation = 0.466 inches.

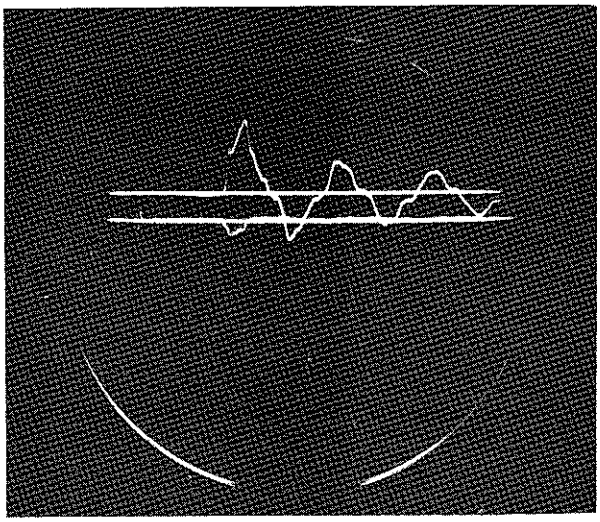

Figure 7a - Current and voltage for P-1 diode with 5-mil tantalum converter

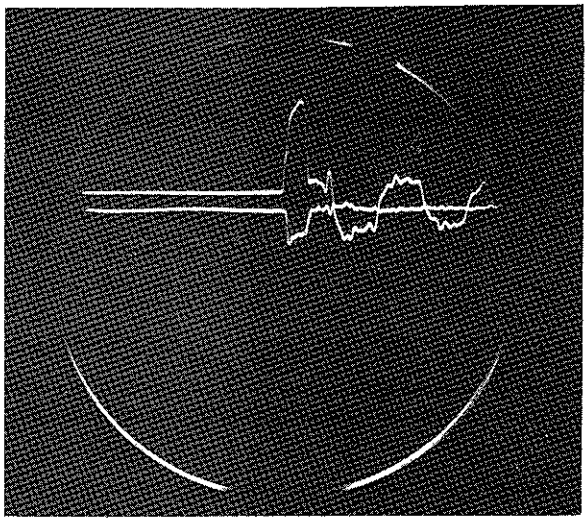

Figure 7b - P-1 diode with 15-mil titanium

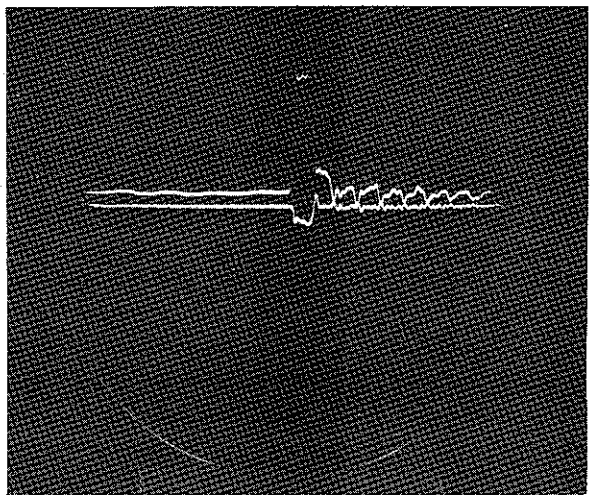

Figure 7c - P-1 diode with 0.125 inch aluminum

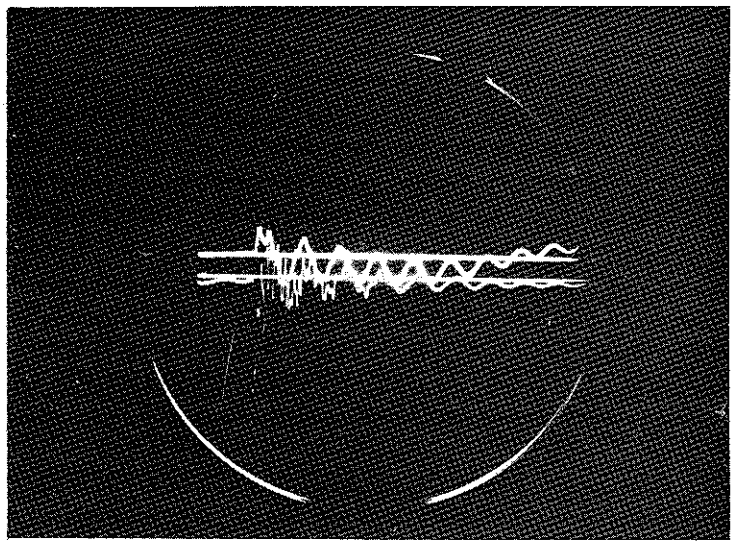

Figure 8 - Current and voltage with P-2 diode and 5-mil tantalum $i_m$ = 23 kA, $v_m$ = 370 kV

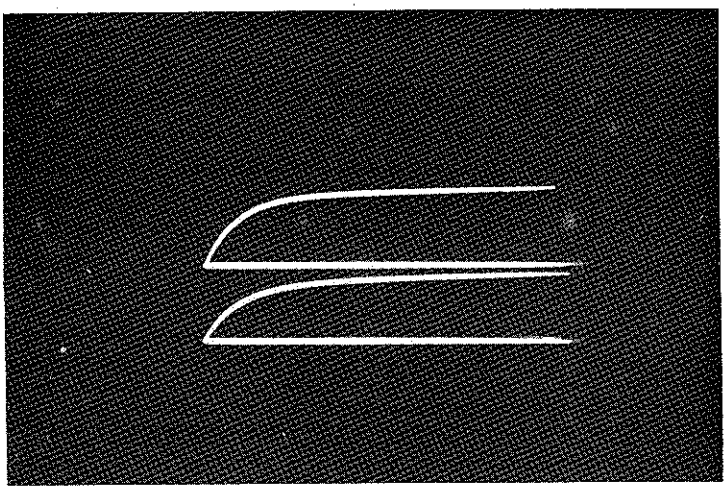

Figure 9 - Signals from identical ionization chambers filled with neon gas to 4 psig and exposed to the same radiation flux. Upper trace - chamber containing very pure gas. Lower trace - chamber containing 1% methyl formate impurity in neon.

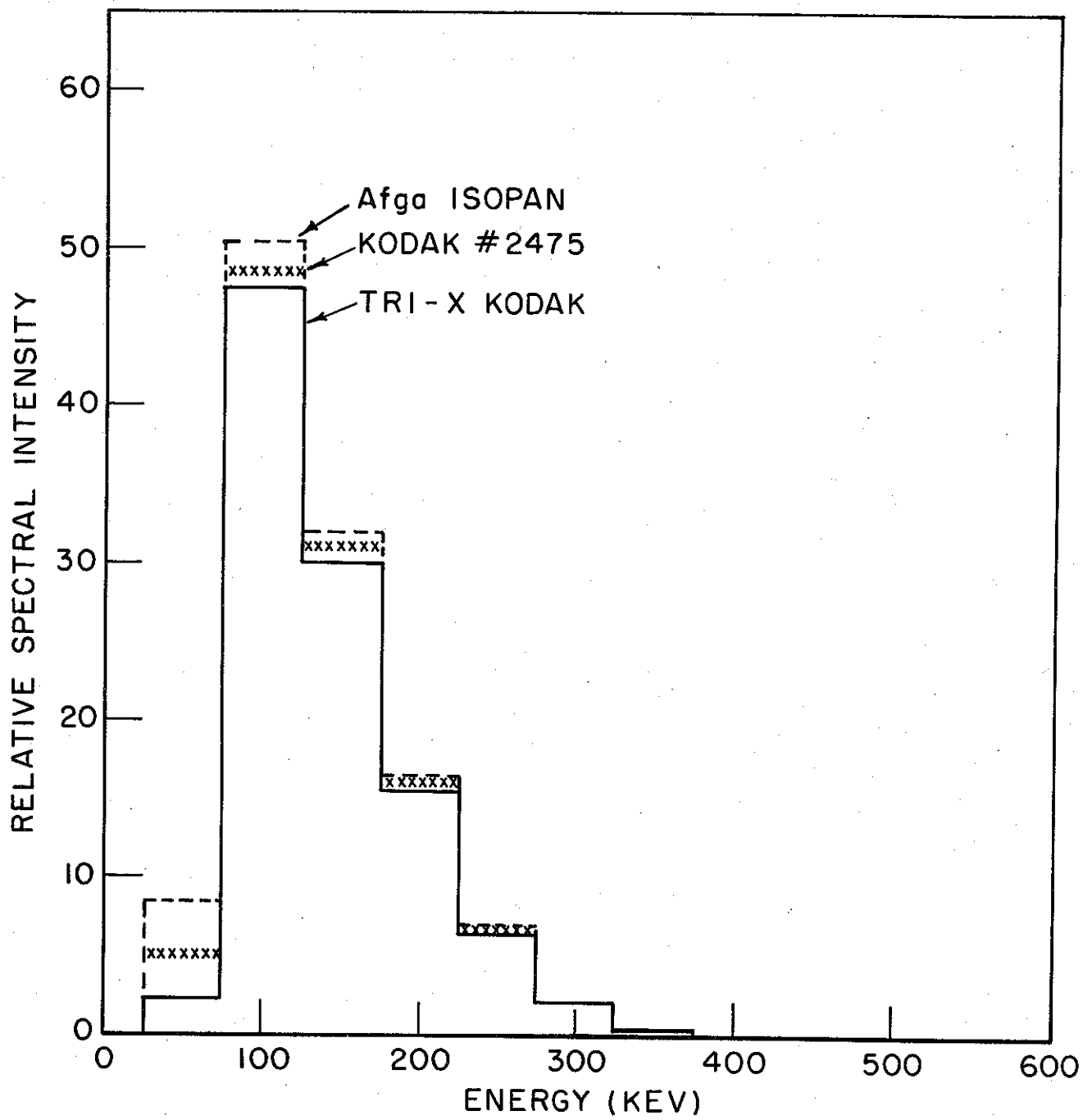


Figure 10 - Comparison of spectra determined from an absorption spectrometer using three types of film as detectors.

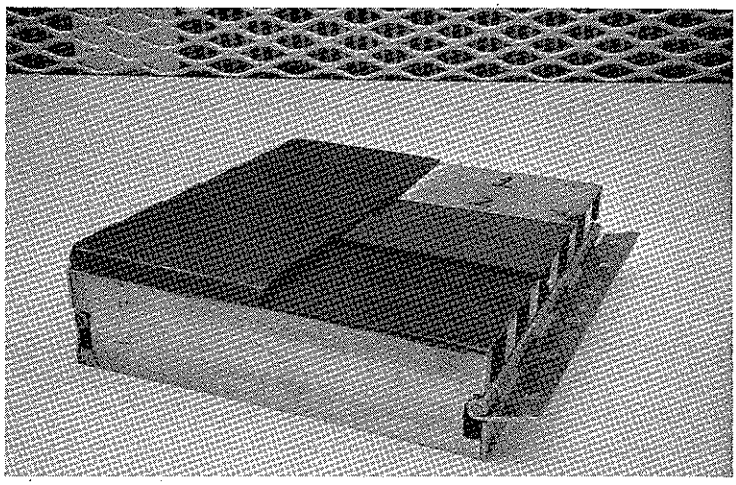

Figure 11a - Box-type TLD spectrometer

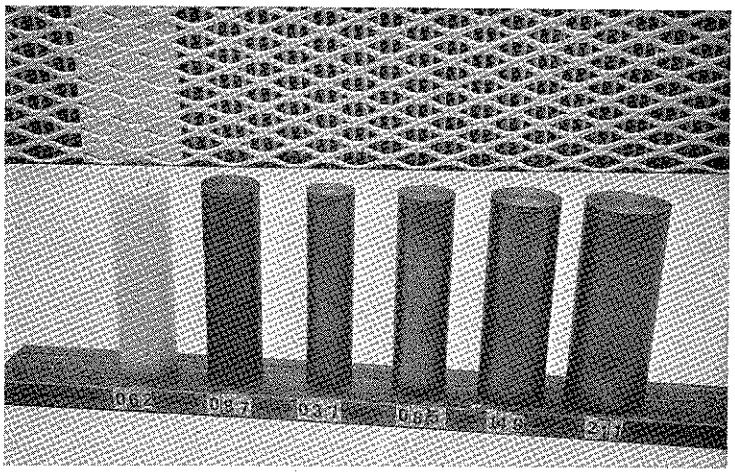

Figure 11b - Cylinder-type of TLD spectrometer

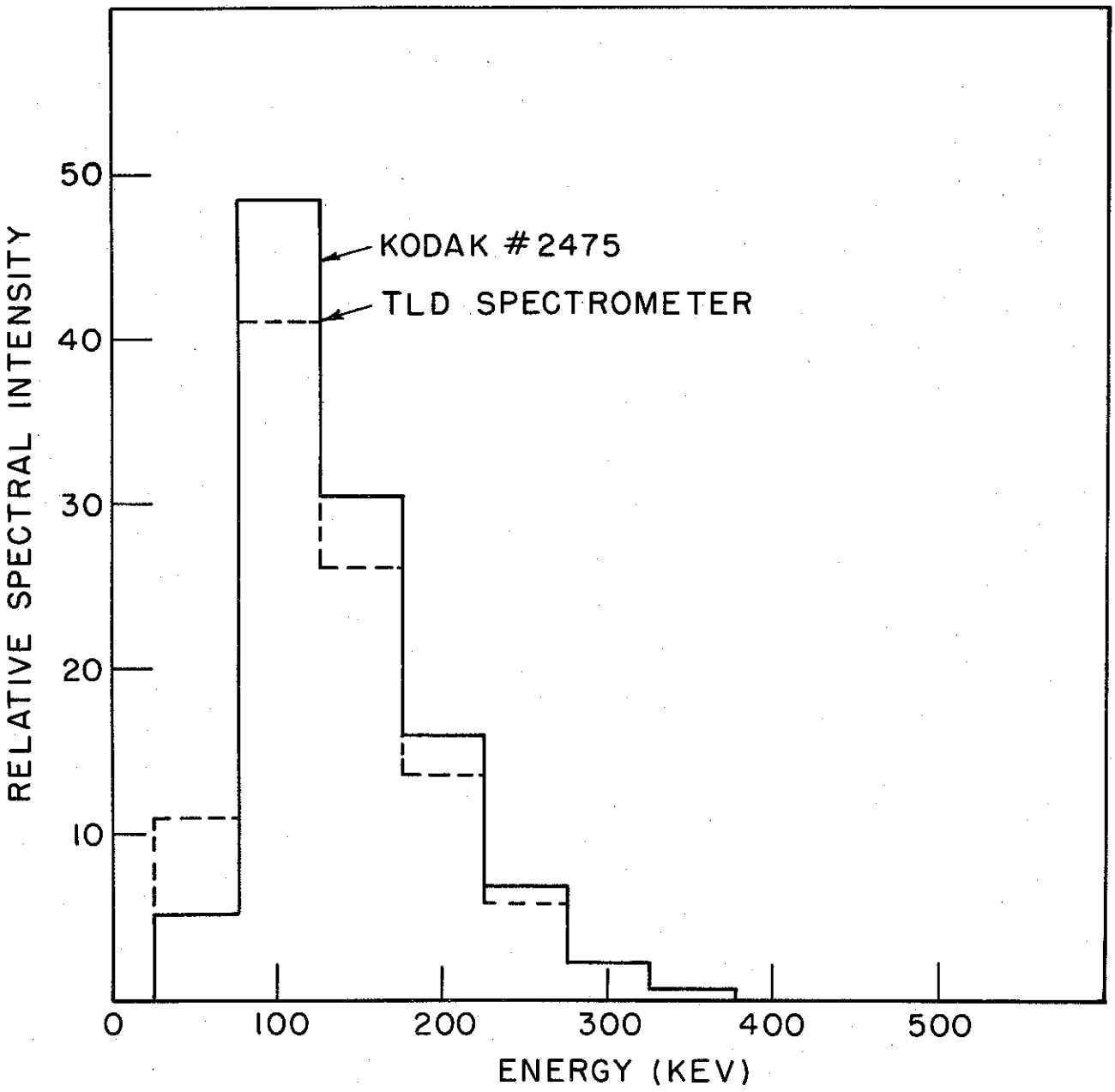


Figure 12 - Comparison of spectra determined from an absorption spectrometer using film and TLD's as detectors.

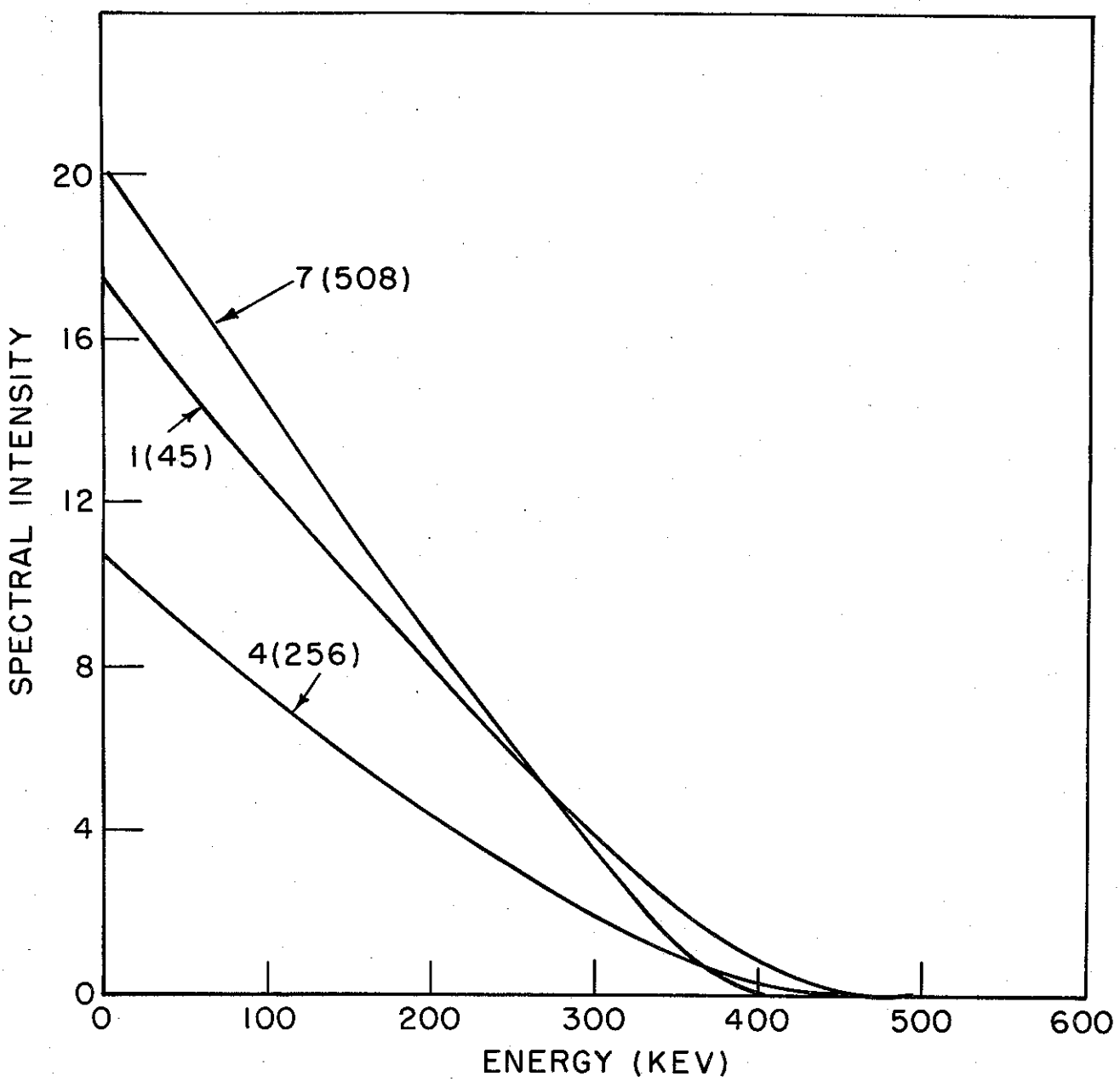


Figure 13 - Unattenuated Kramers spectra for Ti-1 (45), Mo-4 (256), Ta-7 (508)

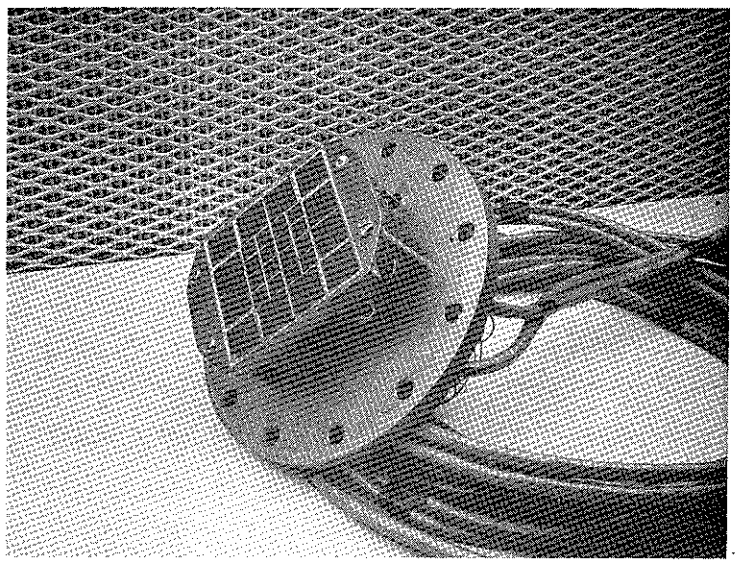

Figure 14a - Carbon block calorimeter for measuring electron beam energy profile

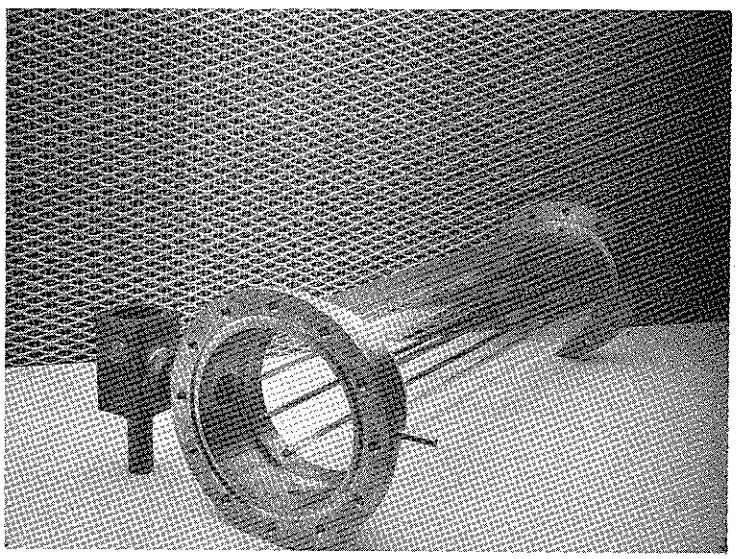

Figure 14b - Drift tube for use in beam diagnostics with the 7-ohm blumlein water generator

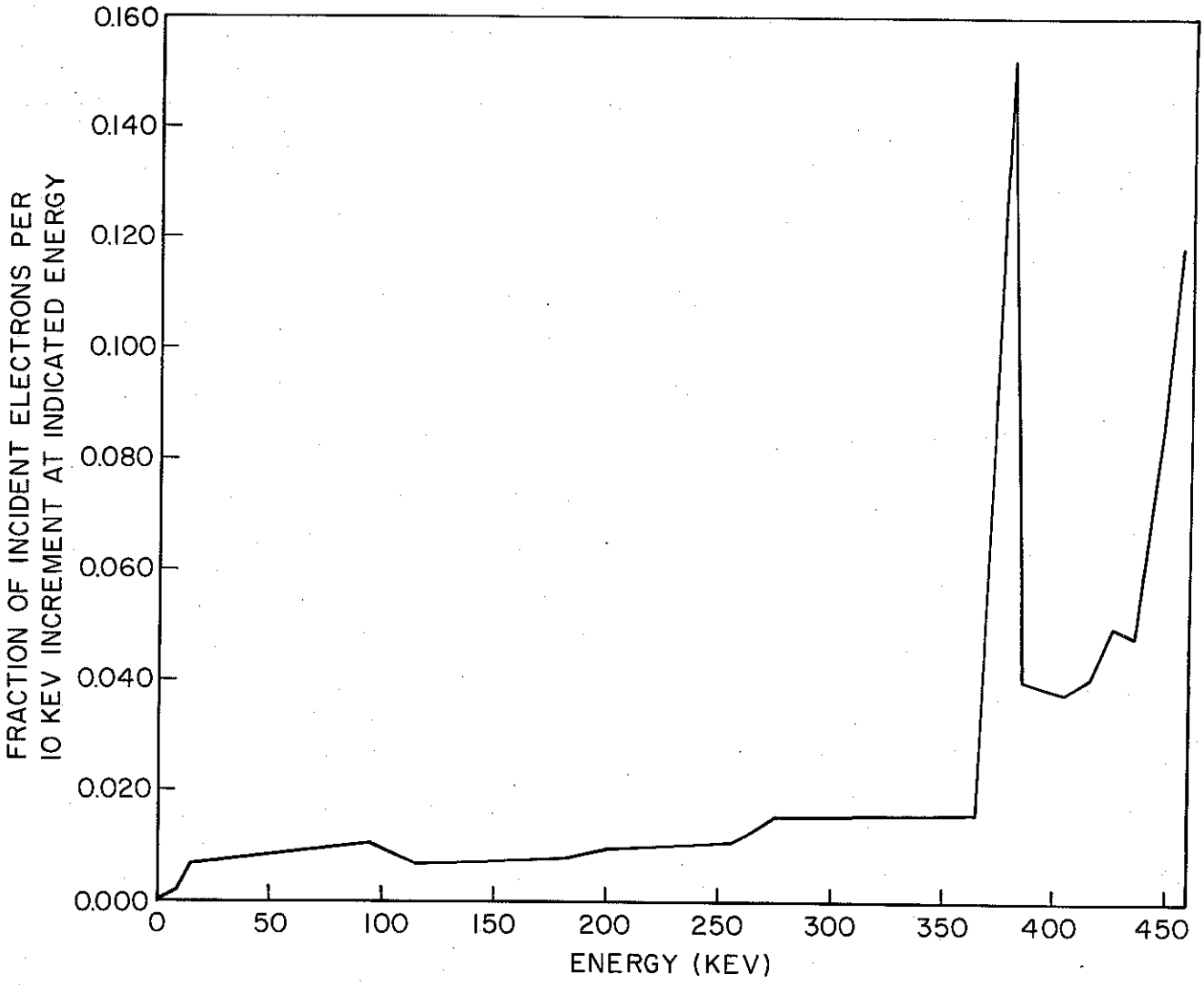


Figure 15a - Primary electron spectrum for Discharge 1 (45) - Titanium anode

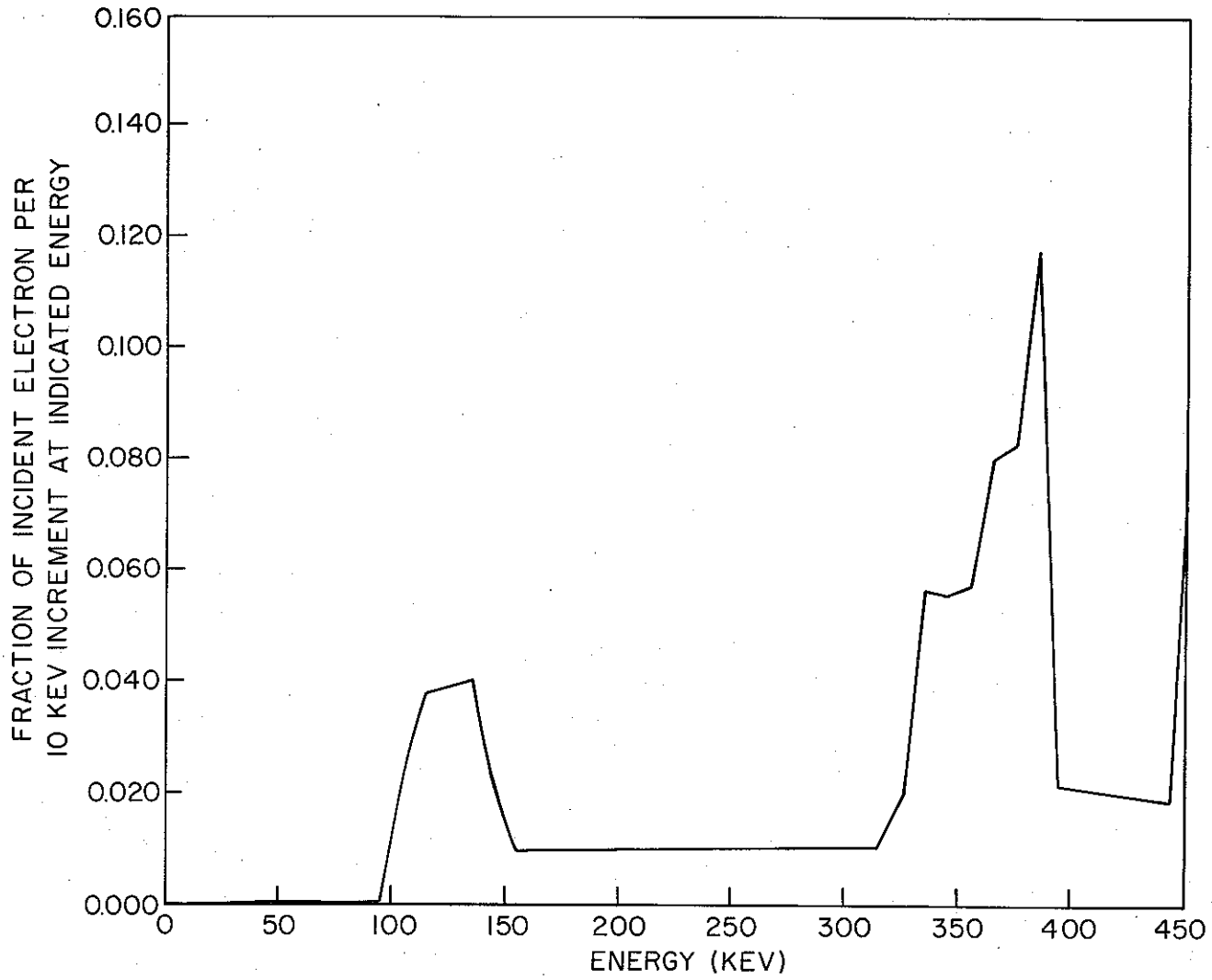


Figure 15b - Primary electron spectrum for Discharge 4 (256) - Molybdenum anode

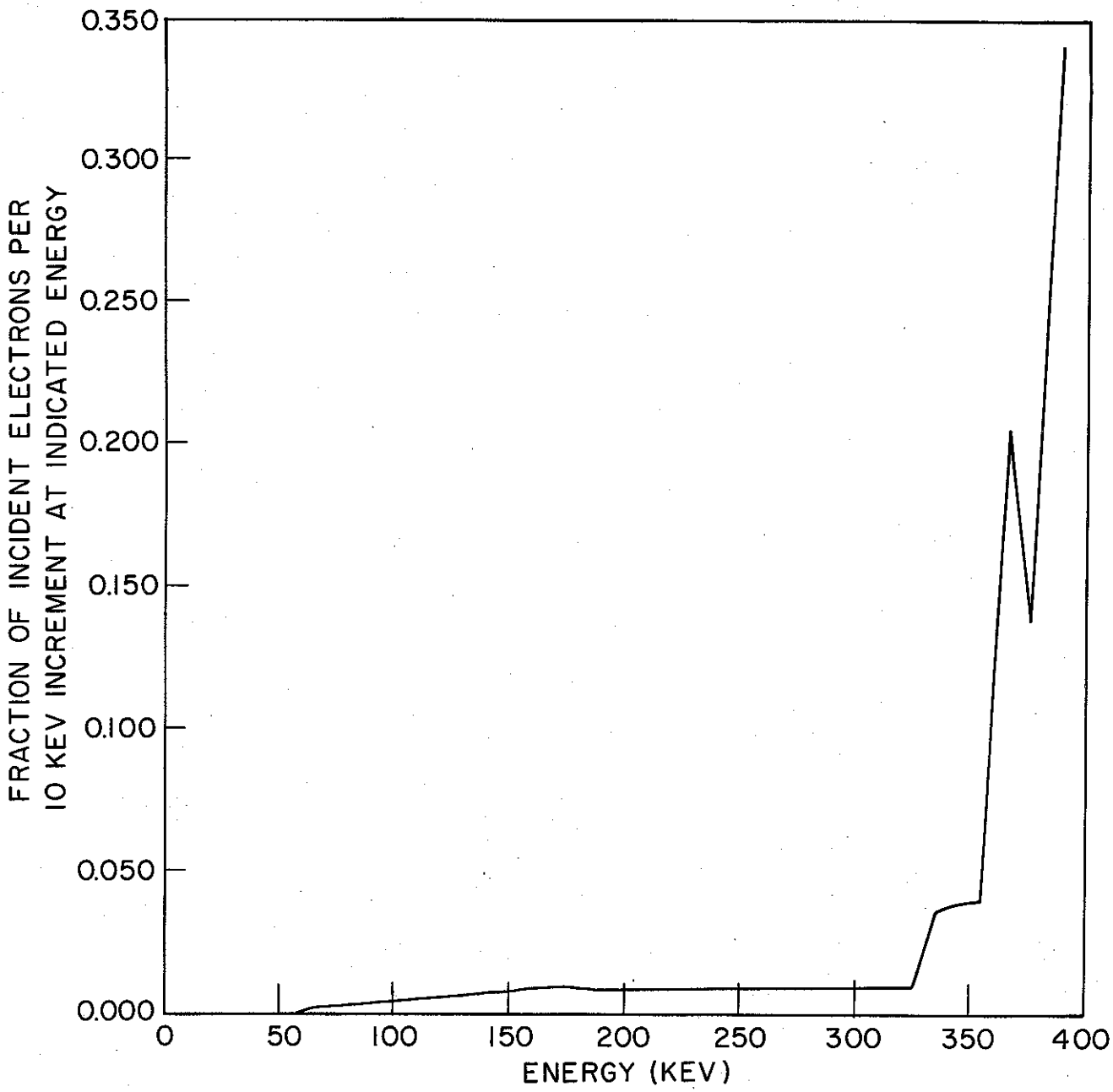


Figure 15c - Primary electron spectrum for Discharge 7 (508) - Tantalum anode

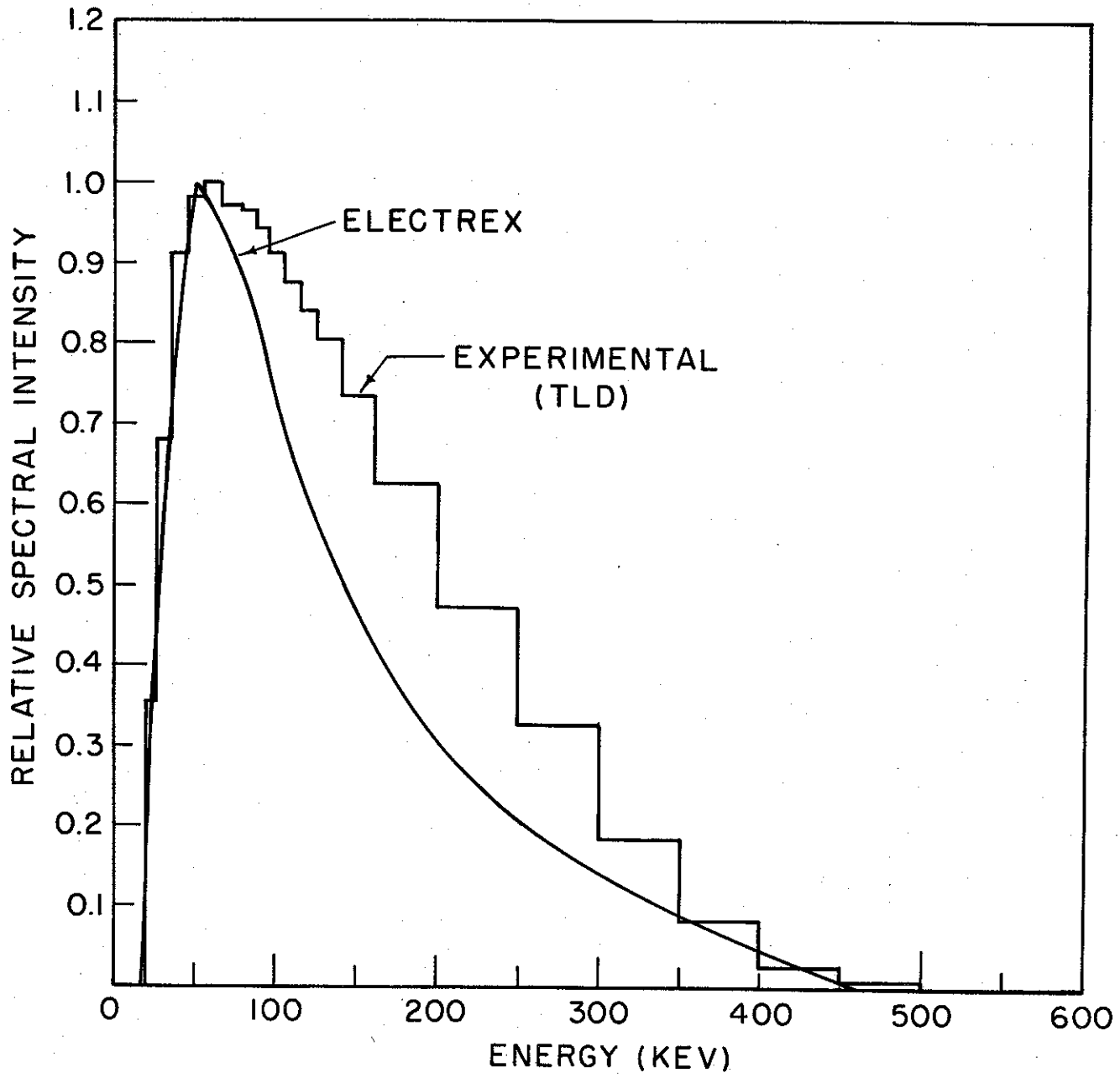


Figure 16 - Comparison of photon spectrum calculated by ELECTREX code and determined from TLD absorption spectrometer for Titanium anode

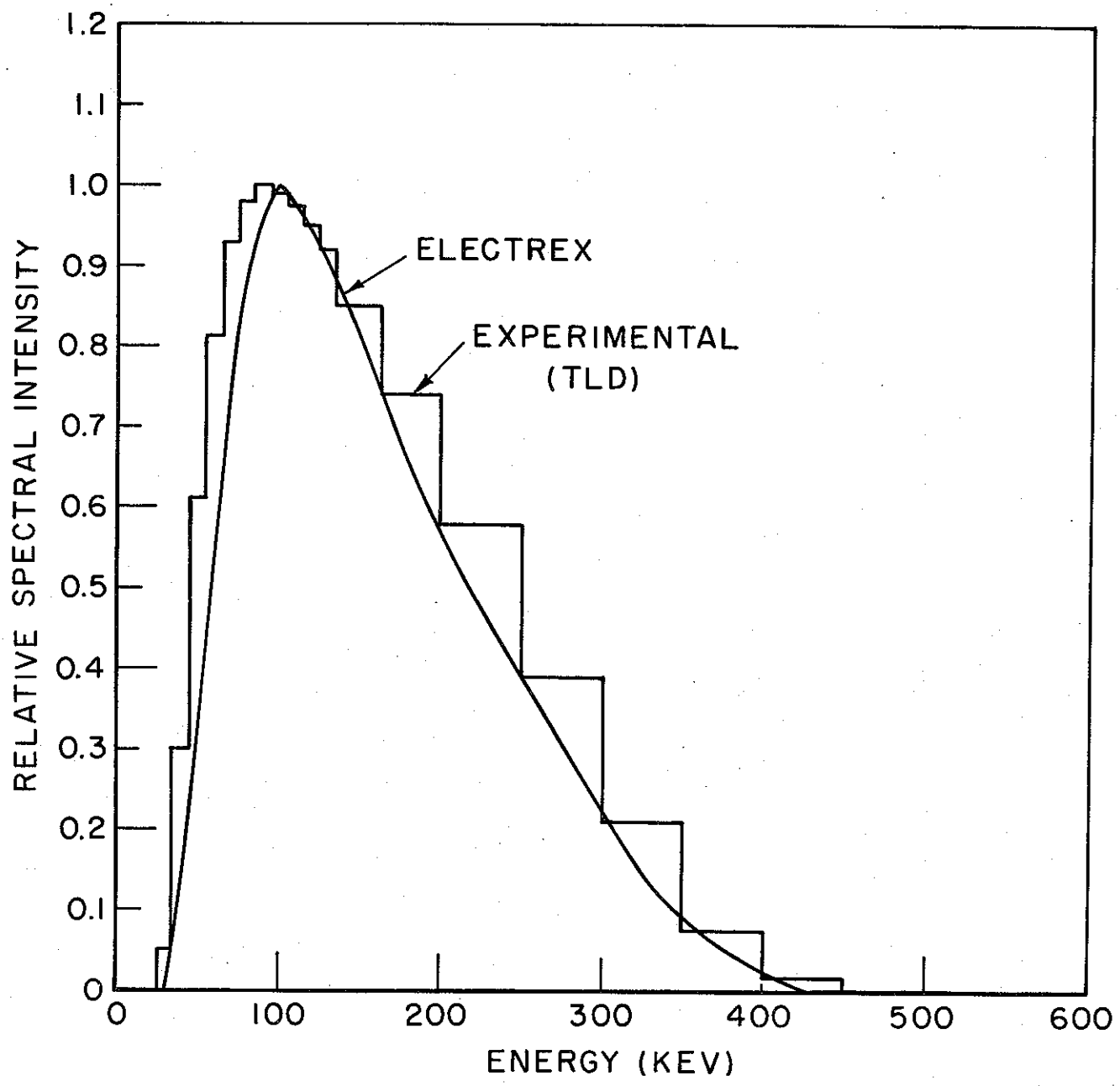


Figure 17 - Comparison of photon spectrum calculated by ELECTREX code and determined from TLD absorption spectrometer for Molybdenum anode

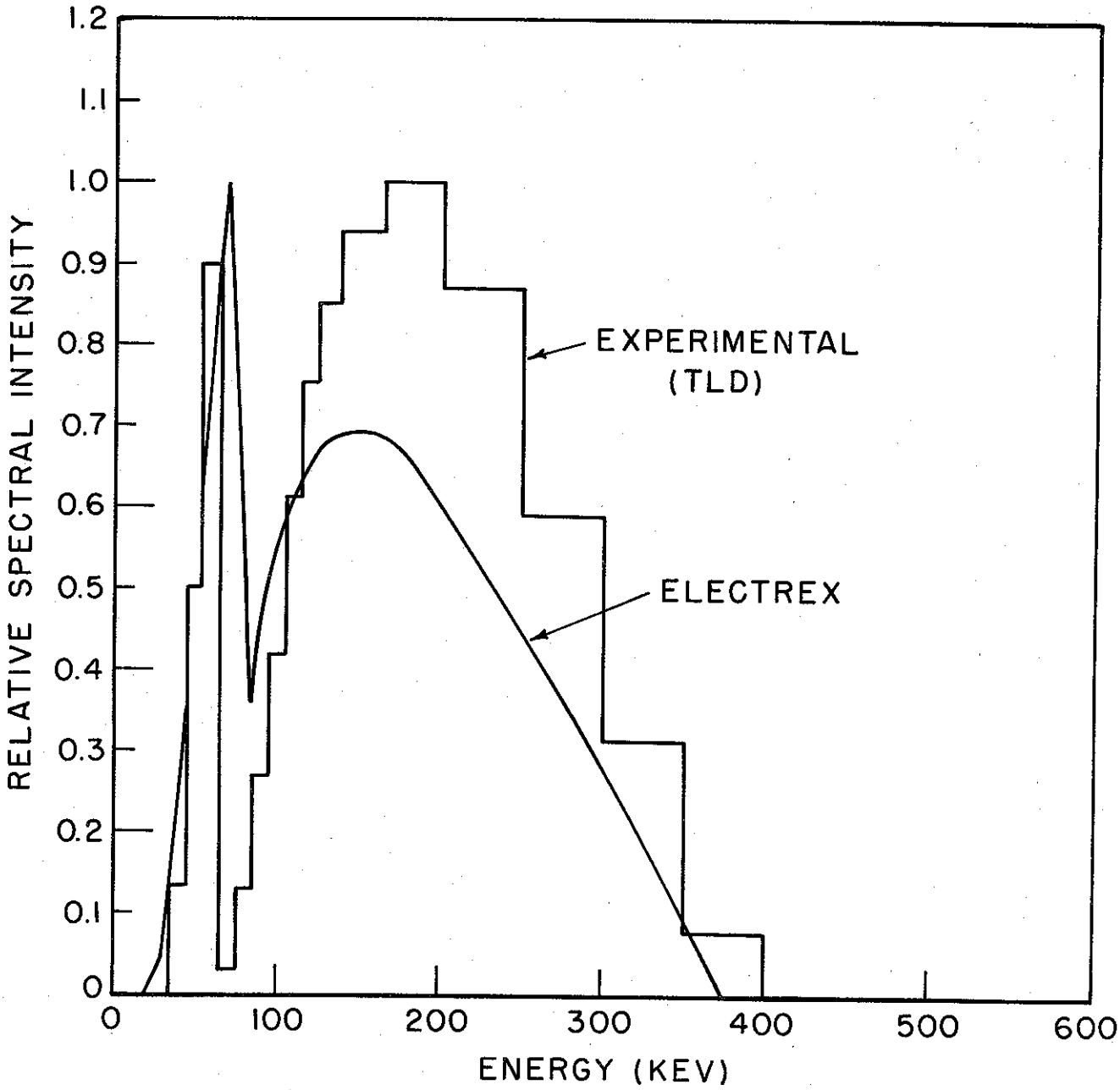


Figure 18 - Comparison of photon spectrum calculated by ELECTREX code and determined from TLD absorption spectrometer for Tantalum

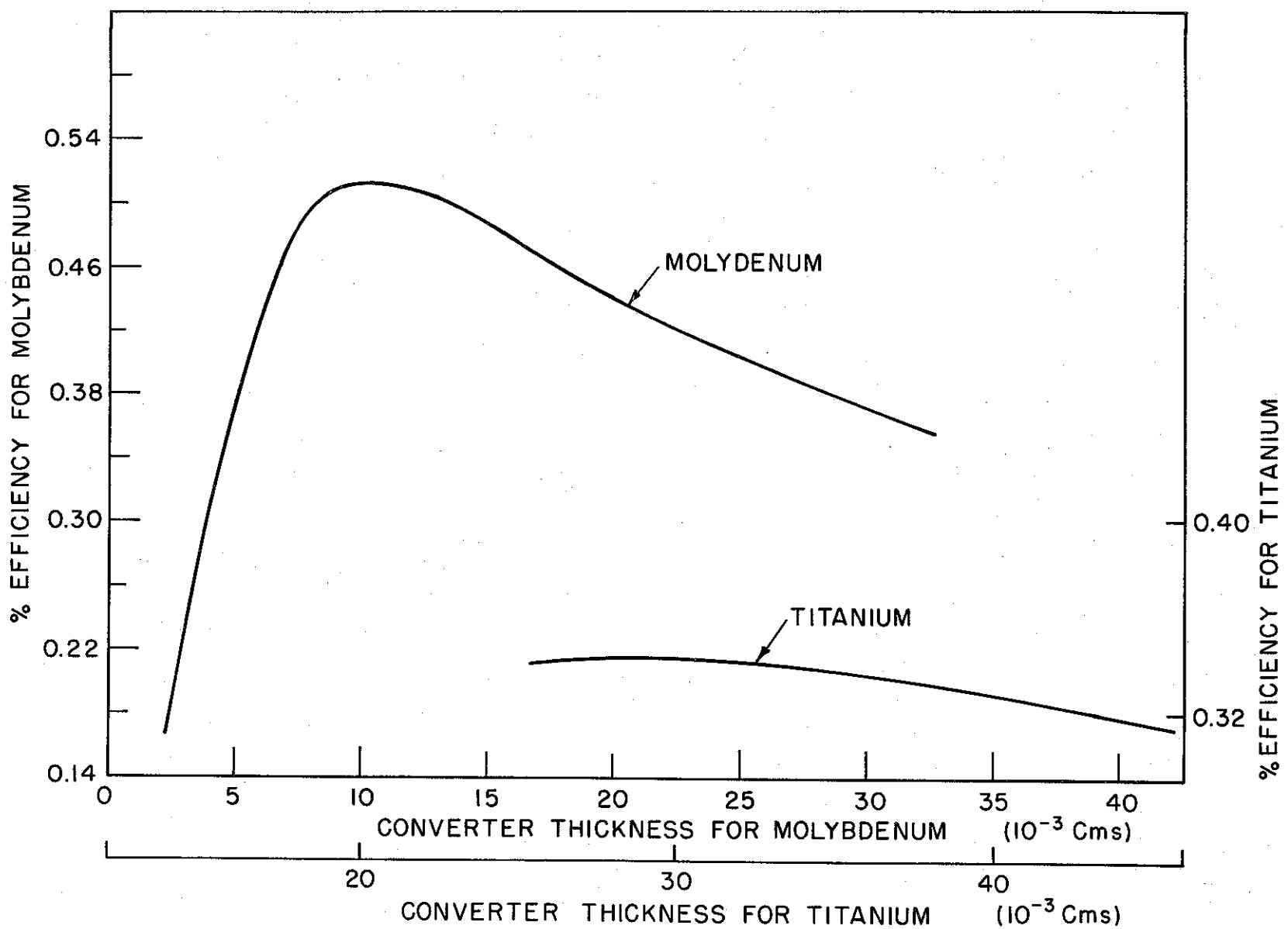


Figure 19 - Calculated conversion efficiency of 500 Kev electrons to photons for various thicknesses of Molybdenum or Titanium anodes

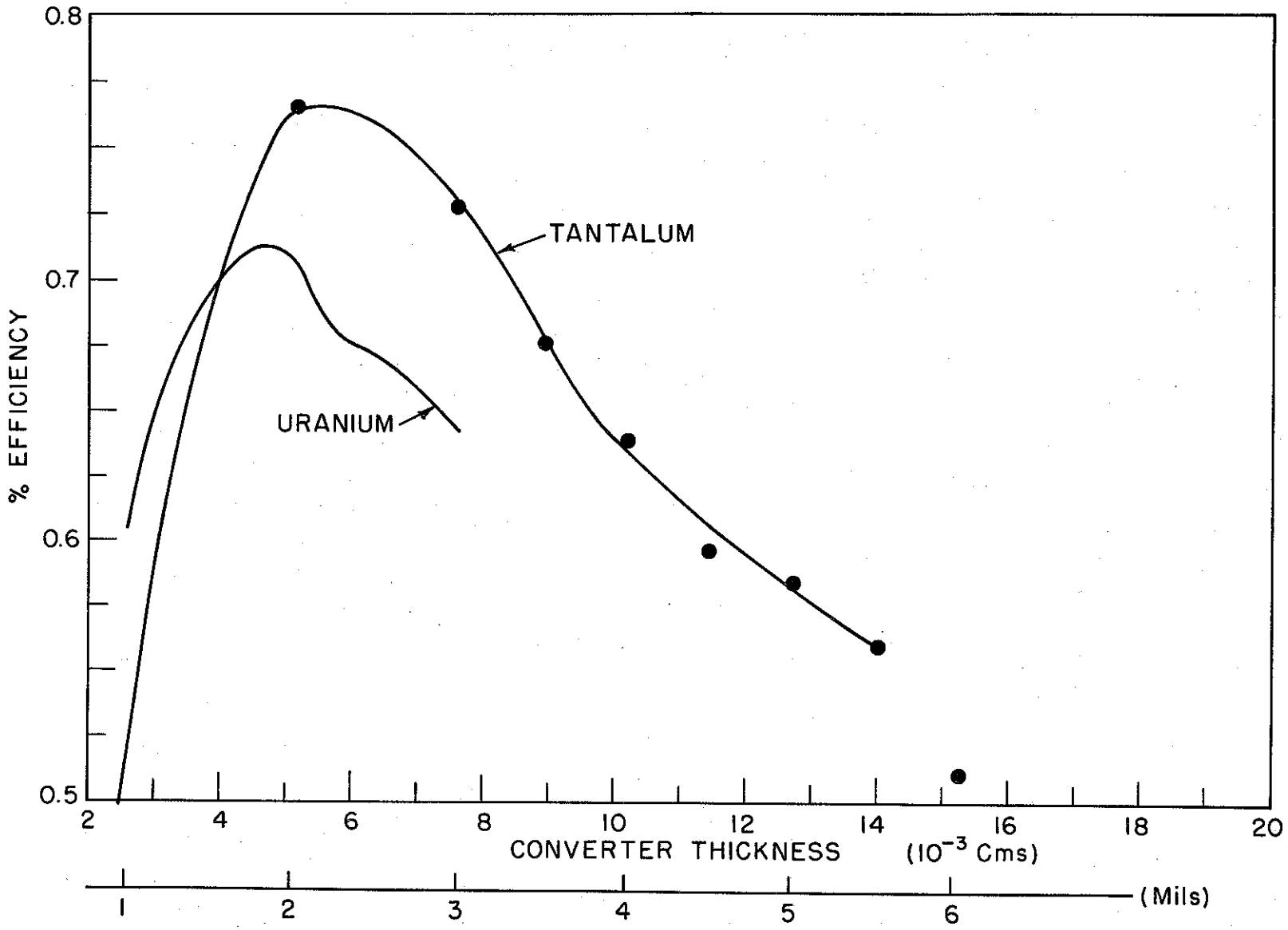


Figure 20 - Calculated conversion efficiency of 500 Kev electrons to photons for various thicknesses of Tantalum or Uranium anodes

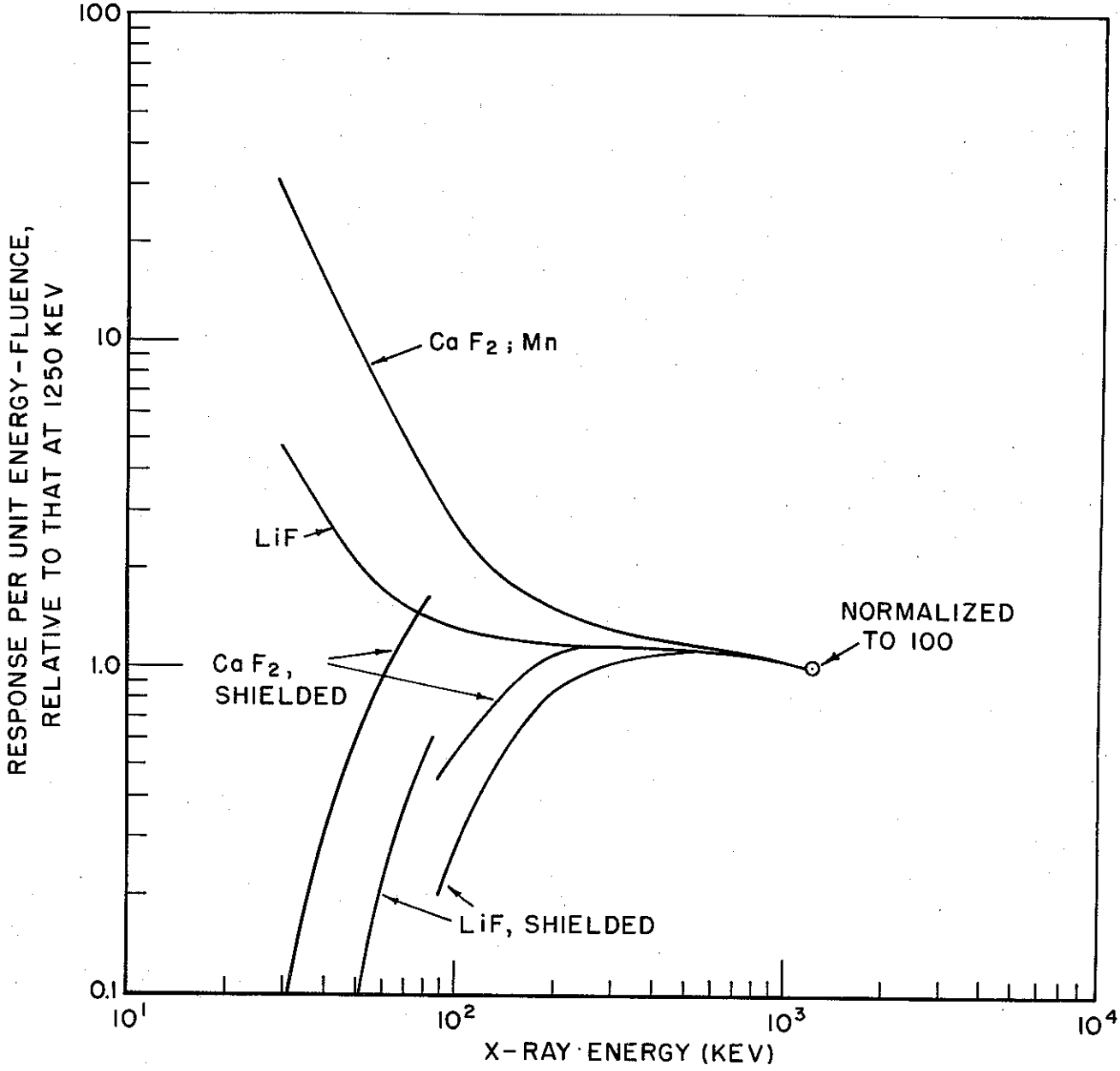


Figure 21 - Response of $CaF_2$ and LiF dosimeters to photons over the energy range of 30 Kev to 1250 Kev